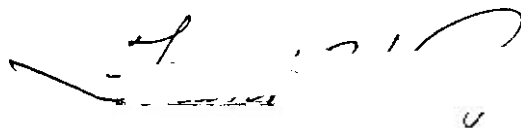


"In presenting the dissertation as a partial fulfillment of the requirements for an advanced degree from the Georgia Institute of Technology, I agree that the Library of the Institution shall make it available for inspection and circulation in accordance with its regulations governing materials of this type. I agree that permission to copy from, or to publish from, this dissertation may be granted by the professor under whose direction it was written, or, in his absence, by the dean of the Graduate Division when such copying or publication is solely for scholarly purposes and does not involve potential financial gain. It is understood that any copying from, or publication of, this dissertation which involves potential financial gain will not be allowed without written permission.

A handwritten signature in dark ink, appearing to be 'L. J. ...', is written below the printed text. The signature is fluid and cursive, with a long horizontal stroke at the end.

MODEL STUDIES OF THE POINT BEARING CAPACITY  
OF FOUNDATIONS IN A COHESIONLESS SOIL

A Thesis

Presented to

The Faculty of the Graduate Division

by

Frank Wintchel Rogers, III

In Partial Fulfillment  
of the Requirements for the Degree  
Master of Science in Civil Engineering

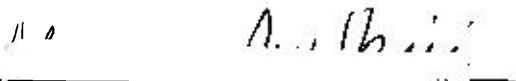
Georgia Institute of Technology

June, 1962


32  
12R

MODEL STUDIES OF THE POINT BEARING CAPACITY  
OF FOUNDATIONS IN A COHESIONLESS SOIL

Approved:

  
Aleksandar Vesic

  
George F. Bowers

  
Radnor J. Paquette

Date Approved by Chairman: May 31, 1962

## ACKNOWLEDGMENTS

The author wishes to express appreciation to Professor Aleksandar Vesic, who provided guidance and encouragement during the course of this work. Grateful appreciation is extended Professors George F. Sowers and Radnor J. Paquette, members of the reading committee, for their many helpful comments on the text. Appreciation is due the Armco Pipe and Metal Products Company of Atlanta, Georgia, for furnishing the soil container used in the project.

To Charles Pavey, highway laboratory machinist, the author expresses gratitude, for he could not have assembled the equipment used in the project without Mr. Pavey's willing help.

## TABLE OF CONTENTS

	Page
ACKNOWLEDGMENTS . . . . .	ii
LIST OF TABLES . . . . .	iv
LIST OF ILLUSTRATIONS . . . . .	v
SUMMARY . . . . .	vii
CHAPTER	
I. INTRODUCTION . . . . .	1
The Problem . . . . .	1
Purpose of Research . . . . .	2
II. REVIEW OF THEORY AND LITERATURE . . . . .	4
III. EQUIPMENT AND INSTRUMENTATION . . . . .	10
IV. PROCEDURE . . . . .	13
V. DISCUSSION OF RESULTS . . . . .	20
Results of Surface Load Tests . . . . .	20
Interpretation of Surface Test Results . . . . .	23
Interpretation of Deep Test Results . . . . .	28
VI. CONCLUSIONS . . . . .	32
VII. RECOMMENDATIONS . . . . .	34
APPENDIX . . . . .	35
Tables . . . . .	37
Illustrations . . . . .	49
BIBLIOGRAPHY . . . . .	73

## LIST OF TABLES

Table	Page
1. Glossary of Abbreviations . . . . .	37
2. Load Settlement Test Results Series I Footings on the Surface.	38
3. Load Settlement Test Results Series I Footings on the Surface.	39
4. Load Settlement Test Results Series I Footings on the Surface.	40
5. Load Settlement Test Results Series I Footings on the Surface.	41
6. Tabular Computation of $N_{\gamma}$ . . . . .	43
7. Load Settlement Test Results Series II Footings Deep . . . . .	45
8. Load Settlement Test Results Series II Footings Deep . . . . .	46
9. Tabular Computation of $N'_q$ . . . . .	48

## LIST OF ILLUSTRATIONS

Illustration	Page
1. Angle of Internal Friction vs Void Ratio . . . . .	49
2. Height of Fall vs Void Ratio Curve . . . . .	50
3. Load Settlement Curves (1 inch Footings) . . . . .	51
4. Load Settlement Curves (2 inch Footings) . . . . .	52
5. Load Settlement Curves (3 inch Footings) . . . . .	53
6. Load Settlement Curves (1 inch Footings) . . . . .	54
7. Load Settlement Curves (2 inch Footings) . . . . .	55
8. Load Settlement Curves (3 inch Footings) . . . . .	56
9. Graph Showing Existence of Cohesion in the Sand . . . . .	57
10. Void Ratio vs Cohesion Curve . . . . .	58
11. Bearing Capacity Factors vs Void Ratio . . . . .	59
12. Results of Surface Plate Load Tests Giving the Bearing Capacity Factor ( $N_\gamma$ ) as a Function of the Angle of Internal Friction $\phi$ . . . . .	60
13. Comparison of $N_\gamma$ Values for Surface Foundations . . . . .	61
14. Load Settlement Curves (2 inch Footings Series II) . . . . .	62
15. Load Settlement Curves (2 inch Footings Series II) . . . . .	63
16. Load Settlement Curves (3 inch Footings Series II) . . . . .	64
17. Load Settlement Curves (3 inch Footings Series II) . . . . .	65
18. Theoretical and Test Values of $N_q$ and $N'_q$ . . . . .	66
19. Comparison of Theoretical $N'_q$ Values . . . . .	67
20. Comparison of Theoretical $N'_c$ Values . . . . .	68

Illustration	Page
21. Large Surface Loading Apparatus . . . . .	69
22. Small Surface Loading Apparatus . . . . .	70
23. Small Lever Apparatus for Deep Load Testing . . . . .	70
24. Apparatus for Conducting Deep Loading Tests . . . . .	71
25. Charging the Bin for a Deep Load Test . . . . .	71
26. Cross Sections Across the Center of the Footing After Failure Has Occurred . . . . .	72



## SUMMARY

The purpose of this investigation was to further the development of the theory of point bearing capacity of foundations on the surface and at great depths in cohesionless soil within the normal range of densities of the soil. The values of the surface bearing capacity factor  $N_\gamma$  and the deep bearing capacity factor  $N'_q$  were to be determined experimentally.

Load tests were conducted to determine the ultimate bearing capacity of one, two and three inch model footings placed on the surface of sand. These surface load tests were run on sands of various degrees of density from loose to dense states.

Load tests were conducted to determine similar ultimate point bearing capacity values for two and three inch footings placed at depths of fifteen diameters. The effect of skin friction was eliminated in the deep load tests by loading the footing through a pipe by means of a lever system and a loading rod which fitted inside the pipe.

Load settlement curves were plotted for each load test and the failure load was taken to be the load corresponding to the settlement just before failure of the footing in dense sand. The settlement just before failure of the footings on the surface was between six and eight per cent of the footing diameter. Thirty-five to fifty per cent of the base width was the amount of settlement needed before failure occurred in the deep load tests.

The results of the tests show that the observed bearing capacity for surface foundations in sand agrees reasonably well with the theory. The bearing capacity factors  $N_\gamma$  found from the surface tests compare favorably with theoretical values and with experimental values from other research.

The observed bearing capacity of deep foundations in sand is considerably less than estimated by the present theory due to the fact that the effect of the compressibility of the material is neglected in the theory. The compression of the sand under the footing does not allow the assumed failure surfaces to develop in loose and medium dense sands; therefore, the theoretical bearing capacity factors derived from the geometry and shear characteristics of the failure surface are not valid for loose and medium sands. The sand appears to be sufficiently incompressible in the dense state for general shear failure to occur and the observed bearing capacity approaches that estimated by the present theory.

It is recommended that further tests be conducted to determine the shape of the failure surfaces for loose to medium dense sands. With this information, theoretical bearing capacity factors, which would be compatible with the results of load tests, could be derived.

## CHAPTER I

### INTRODUCTION

The Problem.--The design of foundations must satisfy two main requirements: namely, the soil beneath the foundation must not fail and the total settlement of the foundation must be kept within limits that can be tolerated by the superstructure. This study is only concerned with the failure of the foundation, or its ultimate point bearing capacity.

The bearing capacity of a foundation on the surface is due only to the base resistance or point bearing capacity of the foundation. The bearing capacity of deep foundations and piles depends upon two parts; point resistance and skin resistance. It is an old problem of foundation design to compute both separately. The point bearing capacity is essentially the bearing capacity of a foundation founded at a very great depth ( $D/B > 5$ ). The skin resistance consists of adhesion and skin friction; however, in cohesionless soils adhesion is negligible. The skin friction is produced by earth pressure acting on the surface of the pile.

In cohesionless material the base resistance increases rapidly with foundation depth and for deep foundations the base resistance is the predominant feature and the skin friction is relatively small.

Since the bearing capacity is an extremely sensitive function of the density of the material, one must be able to determine the density of the soil with a high degree of accuracy. In view of the difficulty

of procuring undisturbed samples of cohesionless soil, the best estimates of bearing capacity are subject to considerable error.

The bearing capacity of footings and piles located below the surface in most cases has not been determined experimentally. In many instances where tests were conducted to measure the point resistance of a pile, the soil was in a dense condition. Theoretical analyses of the problem have been based on the theory of plasticity and on simplifying assumptions due to the complex mathematical difficulties of the problem. One erroneous assumption is that a complete general shear bulb develops for all values of density of the soil involved. This allows a solution of the problem by considering the geometry and shear characteristics of the assumed failure surface for any value of density or angle of internal friction. The values obtained for high degrees of compactness of the sand agree fairly well with the tests performed on dense sands. Owing to the lack of experimental tests on sand of medium and low densities prior to 1951, the bearing capacity of deep foundations on loose sands has been over-estimated by the present theoretical approach.

Purpose of Research.--This work attempts to further the development of the theory of bearing capacity of foundations on the surface and at great depths in cohesionless soil within the normal range of compactness of the soil. Two goals are to be reached by this research. The first goal is to determine experimentally values of the surface bearing capacity factor  $N_y$  for the normal range of densities of the sand. The second goal is to determine experimentally the values of the deep bearing capacity

factor  $N'_q$  for the normal range of densities of the sand. It is hoped that these values will aid in the design of surface and deep foundations.

## CHAPTER II

## REVIEW OF THEORY AND LITERATURE

The problem of bearing capacity of foundations on the surface of cohesionless soils has been studied extensively in the last twenty years. Several different theoretical solutions of the bearing capacity of a foundation on sand have been proposed. Most of these solutions define the bearing capacity in terms of the physical properties of the soil (density, shearing strength, and deformation characteristics), and on the physical characteristics of the foundation (size, depth, shape, and base roughness).

The bearing capacity of surface foundations is generally estimated on the assumption that the soil is homogeneous from the surface to a depth far below the level of the base of the footing.

Terzaghi (1) has shown that the bearing capacity  $p$  of a shallow strip foundation of width  $b$  and depth  $D$  can be represented by the expression:

$$p = cN_c + qN_q + \frac{1}{2}\gamma bN_\gamma \quad (1)$$

where:

$$N_c = (N_q - 1) \cot \phi$$

$$N_q = e^{\pi \tan \phi} \tan^2(45^\circ + \frac{\phi}{2})$$

$$N_{\gamma} = \frac{1}{2} \frac{K_p \sin(45^\circ + \frac{\phi}{2})}{\cos^2(45^\circ + \frac{\phi}{2})}$$

Equation (1) can be adapted to foundations that are not strips by including shape factors which show the ratio of the bearing capacity of a non-strip type of base to a strip type:

$$p = cN_c \xi_c + qN_q \xi_q + \frac{1}{2} \gamma b N_{\gamma} \xi_{\gamma} \quad (2)$$

In the case of a circular base supported on the surface the values of the shape factors are:

$$\xi_c = 1.20$$

$$\xi_q = 1.20 - \frac{0.20}{N_q}$$

$$\xi_{\gamma} = .70$$

In the case of a purely cohesionless soil with the foundation resting on the surface the value of the bearing capacity becomes:

$$p = \frac{1}{2} \gamma b N_{\gamma} \xi_{\gamma} \quad (3)$$

Therefore, it is obvious that the most important bearing capacity factor for a foundation on the surface of a sand is  $N_{\gamma}$ .

Many solutions of  $N_{\gamma}$  have been presented (Fig. 13). These solutions are based on the theory of plasticity and differ mainly in the assumption of the shape of the sliding surface.

Meyerhof (2) made several small scale model tests using rectangular and square base footings. The width of the bases were  $1/2$ " and 1". In his tests he studied the effects of the shape of the foundation on the bearing capacity. He also studied the influence of depth. His results were compatible with values predicted by the theory of plasticity. Meyerhof (3) later introduced some corrections to the values of  $N_\gamma$ .

Probably the most extensive tests to date were made by DeBeer and Vesic (4). These investigators made a large number of load tests on model footings resting on sand. In the tests they varied the unit weight of the sand from maximum to minimum values. In this work values of  $N_\gamma$  were obtained as a function of the angle of internal friction. At the same time DeBeer and Vesic studied the shape of the sliding failure surfaces by placing layers of different colored sand which contained a small amount of cement. After failure had occurred the cement was hydrated by allowing water to seep into the sand. Upon hardening the sample was sawed perpendicular to the longitudinal axis of the footing and the shape of the sliding surface could be noted.

Three types of rupture were noted in the sand: complete rupture, incomplete rupture, and punching. These types of rupture always occurred within well defined limits of densities. The magnitudes of the settlements at rupture were about five to seven per cent of the base widths.

From the tests on the models with subsequent hardening of the cement the Prandtl and Rankin zones were visible.

It was also shown that the values of bearing capacity for rough bases were not significantly different from values obtained for semi-rough bases. This opinion is corroborated by Terzaghi (5). However,



Meyerhof (6) found that a perfectly smooth base theoretically decreases the bearing capacity by one-half.

There is not as much existing research concerning the bearing capacity of deep foundations on sand. Jaky (7) observed that the point of a pile is surrounded on all sides by soil, and there is no obstacle to prevent the sliding surface from developing right up to the surface of the pile in an inverted heart shaped type of figure.

He generalized the Prandtl theory and neglected the unit weight of the soil in his analysis. The result of his analysis gives the value  $N'_c$  as:

$$N'_c = \cot \phi \tan^2(45^\circ + \frac{\phi}{2}) e^{2\pi \tan \phi} - 1$$

Values of  $N'_c$  are plotted in Fig. 20.

Meyerhof (8) presents probably the most comprehensive study to date. In the first part of his article he develops the theory of bearing capacity, on the basis of plastic theory.

$$q = cN'_c + qN'_q + \frac{1}{2}\gamma bN'_\gamma \quad (4)$$

where:

$$N'_c = \cot \phi \left[ \frac{(1 + \sin \phi) e^{2\theta \tan \phi}}{(1 - \sin \phi) \sin(2\eta + \phi)} - 1 \right]$$

$$N'_q = \frac{(1 + \sin \phi) e^{2\theta \tan \phi}}{(1 - \sin \phi) \sin(2\eta + \phi)}$$

$$N'_\gamma = \left[ \frac{4K_p \sin(45^\circ + \frac{\phi}{2})}{\gamma b^2} - \frac{1}{2} \tan(45^\circ + \frac{\phi}{2}) \right]$$

To avoid calculating these values of  $N'_c$  and  $N'_q$  in every case, they have been plotted in Figs. 19 and 20.

In the second part of his article he presents the results of laboratory and field load tests. His tests show that the observed bearing capacity of shallow foundations in sand is in reasonable agreement with theoretical predictions. For deep foundations, however, the actual bearing capacity is considerably less than estimated. For dense sand general shear failure usually occurred. The mechanism of failure was similar to that assumed in the theory, and the extent of the rupture surface was much greater for strip than circular foundations. For loose sand local shear failure occurred without noticeable rupture surface. The bearing capacity of loose sand was considerably less than estimated in deep foundations. This was thought to be caused by the compressibility of the material leading to incomplete formation of the expected sliding surface resulting in local shear failure. Meyerhof also investigated the effect of the shape of the base on the bearing capacity of deep foundations, and noted that the bearing capacity increases with smaller ratios of base to width for deep foundations and is a maximum for a circular base. Driven foundations were also found to have bearing capacities less than was estimated, but the difference was smaller than for buried foundations. This was found to be especially true when loose sand was used, because the influence of the compressibility of the material was partially offset by the increased density after installing the foundation.

For special cases Jaky's and Meyerhof's values of  $N'_c$  are the same.

Caquot and Kerisel (9) have proposed a value of  $N'_q$  for deep foundations:

$$N'_q = 10^{3.04 \tan \phi}$$

$$N'_c = (N'_q - 1) \cot \phi$$

These values are also plotted in Figs. 19 and 20.

## CHAPTER III

## EQUIPMENT AND INSTRUMENTATION

In both the surface tests and the deep tests, which are entitled Series I and Series II, footings of various diameters were used to show the effect of small scaled footings used in the tests. The model footings used in the surface tests consisted of one inch, two inch, and three inch circular models made of steel plates. On the top of each model footing an indentation was machined in the shape of a hemisphere to accept a steel ball bearing which assured that the load was transferred from the loading device to the footing evenly in all cases. A sheet of emery paper, which assured a rough base, was glued to the bottom of each of the footings. Although recent tests by DeBeer and Vesic (10) show that the bearing capacity is only increased by approximately ten per cent at high values of the unit weight of the sand, it was felt that it would be best to use a rough base since Meyerhof (11), in his tests, showed that the difference between a semi-rough base and a rough base was significant.

The containers used in both the surface and deep tests consisted of three foot sections of Armco corrugated metal pipe. This type of container was sufficiently rigid to prevent any lateral deformation while the tank was being loaded. Such lateral deformation would change the density of the sand.

The surface load tests were accomplished by using two loading apparatuses. The first consisted of a small rod and weight platform

connected through a micrometer dial gauge and was used in testing the one inch footings on loose sand. As the load was placed on the platform, the micrometer would register the deflection directly. This apparatus is shown in Fig. 22. Since the failure load for the two and three inch footings was between fifty-three and one hundred and seventy pounds, a stronger loading device, similar in principle to the first, was constructed using steel plates and angles. A micrometer dial gauge connected to the bin measured the deflection. This apparatus is shown in Fig. 21.

The deep loading devices consisted of a steel loading frame, which extended above the container and was attached to the base. A lever system was used to load the foundation. The foundation was loaded through a pipe which eliminated the effect of skin friction on the bearing capacity of the base. The load was transmitted to the foundation by a steel rod which had a ball bearing welded to its end. In each case the steel rod was not lowered directly onto the foundation. The rod was connected to the loading head and as the loading arm was lowered, the weight of the loading rod was gradually transferred to the foundation.

There were two lever systems used in the deep load tests. The first and smaller lever, shown in Fig. 23, consisted of a piece of flat aluminum stock four feet in length and was used to load the footings in the loose and medium dense conditions. The second lever system, shown in Fig. 24, used in the dense conditions, consisted of a fifteen foot T beam fashioned from one inch steel stock. Lead weights were used to apply the load. The large lever arm was counterweighted so that upon

centering the loading head on the loading shaft there were only one hundred pounds applied to the footing. This included the weight of the loading shaft and was determined by placing a scale under the loading shaft. The effect of friction in the loading apparatus was checked by adding weights to the lever and weighing the load produced at the lever shaft. In all cases involving the large lever system the load produced was equal to ten times the load added plus one hundred pounds. The small lever arm was not counter weighted and the load produced at the loading shaft was found to be four times the load added plus twenty-two pounds.

The other item of special equipment used during this study was the container which supplied the sand to a nozzle arrangement used in placing the sand in the tank. This consisted of a fifty-five gallon barrel to the bottom of which a three inch water hose was attached. On the end of the water hose was a flared nozzle; the diameter of the nozzle at its flared end was six inches. The sand was poured from the nozzle through a sieve arrangement of holes one eighth inch in diameter. An illustration of the barrel and hose appears in Fig. 24. It was found that the size and spacing of the holes affected the void ratio obtained from dropping the sand from the various heights. The size of the holes used did not give a large variation in void ratios as the height was varied, but it was found that in using smaller diameter holes the sand would not flow freely from the container and the density was affected. The fifty-five gallon barrel, used for filling the test bin, was raised above the bin by means of a crane. The barrel which supplied the sand through the flared nozzle could be maintained at any desired elevation by the automatic control affixed to the crane.

## CHAPTER IV

## PROCEDURE

Preliminary Tests.--Before the main loading test could be run, certain preliminary tests were made. First, a sample of the sand to be used in the load test was dried and a series of triaxial shear tests were run on the sample. Each sample was prepared by dropping the sand from a sieve-like container into the membrane, which was held in the forming mold, from various heights. These heights varied from zero to thirty-two inches. After the sand was dropped into the mold, the cap was applied to the top of the specimen. The specimen was then carefully placed in the loading machine. The confining pressure applied to the sample was applied by a vacuum pressure pump. This pressure could be measured by a vacuum gauge connected to the specimen. The load tests on the specimen were run in a continuous strain device at the rate of 0.005 inches per minute. The triaxial test was performed according to standard procedures. The results of the triaxial shear tests are plotted in Fig. 1 which show the angle of internal friction as a function of the void ratio.

The sand to be used in the model tests was first dried and placed in a storage bin. The drying was accomplished by first placing the damp sand in sacks and then putting the sacks of sand in a heat room which was maintained at a temperature of about 130°. After approximately two days, the sand was removed and placed in the storage bin.

Tests to calculate the variations in density with respect to the height of drop were run on the sand. First, small scale tests were run in a one cubic foot container which could be continually weighed on a scale. The same nozzle arrangement which was used to drop the sand into the larger bin was used in this test. The calibration consisted of dropping the sand from zero, four, eight, sixteen, and thirty-two inches, and then weighting the sand after each successive drop. After performing the tests on the one cubic foot bin it was thought advisable to perform tests on the full-size container. This was done by first lifting the full-size container onto a platform type scale, and the sand was then poured from the storage bin into the test bin from heights of zero, four, eight, sixteen, and thirty-two inches. Again the unit weight of the sand in the container could be determined from the weight and volume relation. The effect of the different sizes of containers can be seen in Fig. 2. Notice that for the series of drops made in the triaxial shear tests the void ratios at each increment of height are smaller than the void ratios for the full size and one cubic foot tests. The cause of this difference is thought to be aerodynamic. It can also be seen in Fig. 2 that for the full size tests there is little change in the void ratio when the sand is allowed to drop from a height of more than sixteen inches. However, there is a decrease of void ratio of about 0.06 between zero, eight, and sixteen inch drops. The void ratio can be changed to unit weight in pounds per cubic foot by:

$$\gamma = \frac{G_s \times 62.4}{1 + e}$$



The unit weights obtained from each height of drop of the sand were checked many times and the results were reproduced with small variations. This was a very important factor because the bearing capacity is a sensitive function of the angle of internal friction which varies with the unit weight of the sand. If the results had been difficult to reproduce the values of the bearing capacity factors would have been subject to great error.

A truly dense condition of the sand could not be obtained by dropping the sand; increasing the height of fall more than thirty-two inches did not increase the unit weight of the sand appreciably. In order to obtain a dense sample the sand was compacted in two inch layers by means of a hand tamper. The unit weight of the dense sand was determined by a sampling method which consisted of inserting a sharpened ring into the sample and then removing the sand from around the edges of the ring; then, another sharpened plate was inserted cutting the sand off at the base of the ring, thereby a sample of known volume was secured. The sample could then be weighed and the unit weight obtained from the weight-volume relationship.

Load Testing Program.--The load testing program consisted of two series of tests. Series I is confined to the load tests on surface foundations. Series II consists of load tests on deep foundations. In Series I two tests were run on each diameter of footing with the density of the sand varying from loose to dense. The loose condition was obtained by dropping the sand from a height of zero inches. This corresponded to a void ratio

of 1.07. A void ratio between loose and medium dense was obtained by dropping the sand from a height of eight inches. This resulted in a void ratio of 0.92. The medium dense condition was obtained by dropping the sand from a height of sixteen inches. This resulted in a void ratio of 0.86. The height of drop of the sand was maintained constant by attaching a plumb bob to the nozzle and setting the lengths of the string holding the plumb bob so that the distance from the nozzle to the point of the plumb bob could be either eight or sixteen inches. Then, as the sand was placed into the test bin, the point of the plumb bob was allowed to come in contact with the surface of the sand, thereby assuring that the height of fall remained constant until the bin was loaded. The loading of the bin is illustrated in Fig. 25.

The dense condition was obtained by tamping the sand with a hand tamper in two inch layers. After the sand had been placed in the test bin to the surface of the bin, the surface was struck off smooth by means of a sharpened plate. The excess sand was then removed and placed back in the storage bin. After leveling the surface, the model footing was then placed in the center of the container, care being taken to place the model gently into contact with the surface of the sand. Next, the loading device was assembled and the micrometer dial gauge was brought into contact with the top of the footing. The micrometer dial gauge was set to zero and placed on top of the footing before the ball bearing and loading rods were brought in contact with the model foundation. Upon placing the loading rod on the model, a deflection was read on the micrometer dial gauge and recorded as the initial deflection. This deflection

depended upon which loading apparatus was used. The amount of load caused by the loading apparatus used for the one inch footing was 41.6 grams. The weight of the loading apparatus used for the two and three inch footings was 0.60 pounds. After the loading apparatus was brought into contact with the footing, loads were placed on the footing in even increments and the footing was allowed to settle until settlement practically stopped. In each case the footing was loaded with about ten per cent of the expected failure load. The loading and recording of settlement was continued at this uniform rate until the failure load was approached, then the loading rate was reduced until failure occurred. After failure, the final settlement was measured and any deformation of the surface of the sand adjacent to the foundation was measured. After all measurements were made, the loading apparatus and the footing were removed and the sand was then shoveled back into the storage bin. If any uneven or unbalanced settlement was noticed, such as one side of the model settling more than the other, the results of this test were recorded, but were not used in the computations. In these cases the load test was run again so that only failure by even settlement was used in computing the bearing capacity of the model.

Series II tests on deep foundations were run on two and three inch model footings each placed at depths of fifteen diameters. It was apparent that the close agreements between each pair of identical surface tests eliminated the necessity of repetitious tests; hence, only single tests were conducted on the deep foundations at each value of void ratio. The elimination of these repetitious tests was of considerable importance in

order to economize on the time required to charge the bin, run the test, and remove the sand. The time thus saved was more than two days on each test. However, two and sometimes three tests were run for the dense condition of both the two and three inch deep footings to determine the settlement of the footing just prior to failure. In some cases an excessive settlement on a sample was encountered; and the test had to be repeated sufficiently to establish the correct bearing capacity of the sand. In the Series II tests, the void ratio used for each test was the same as those used in Series I. The two inch footing was tested under loose, loose to medium dense, medium dense, and dense conditions. The three inch footing was tested under the same conditions.

The test program consisted of first bringing the sand to footing level, then the footing and the pipe, which protected the loading rod from coming into contact with the sand were placed at that level. A piece of masking tape was placed around the footing and pipe juncture to prevent sand from entering into the space between the sleeve and the outside of the pipe. This step prevented friction from developing between the sand and the two surfaces. After the pipe was bolted in situ, the sand was placed in the container, loading the container to its surface. The surface was struck off with a sharpened piece of angle. The micrometer dial gauge was set at zero and brought into contact with the loading rod. Next, the lever device was gently lowered onto the loading rod and brought into equilibrium. The deflection resulting from placing the lever device on the loading rod was read and the footing was then loaded in even increments. After each increment of load, the footing was allowed to

settle until the settlement had practically ceased; then the next increment was placed on the lever device. This uniform increment of load, which was approximately ten per cent of the expected failure load, was continued until the failure load was approached; then the increment of loading was reduced until the failure occurred. In the case of a deep foundation, no observed deflection of the surface was noted for any of the tests. After failure occurred, the loading device was unloaded and removed from the loading rod; then the sand was removed from the container and returned to the storage bin.

## CHAPTER V

## DISCUSSION

## General Comments

The purpose of this work was to study the point bearing capacity of a foundation in a cohesionless soil. This discussion will consist of four parts: first, a report of the surface load tests of Series I; second, an interpretation of significant test results from Series II; third, a report of the deep load tests of Series II; and fourth, an interpretation of the test results of Series II.

## Results of Surface Load Tests

Tables 1, 2, 3, and 4 give load settlement results for Series I tests. Load settlement curves corresponding to these tests are presented in Figs. 3, 4, 5, 6, 7, and 8.

Surface Tests in Dense Sand.--Terzaghi (12) defines two limiting types of failure in real soils. The first, general shear failure, is characterized by a load settlement curve with a sudden and well defined passage into failure. This type of failure occurs in compact soils with little compressibility and small strains at failure. In a load settlement test on a dense sand each increment of load added produces a proportional amount of settlement. The load settlement curve is practically a straight line in this first portion before failure occurs. Figs. 6, 7, and 8 illustrate this type of curve. As soon as the failure load is reached

the footing settles suddenly and the amount of settlement is no longer proportional. This is represented by a sharp drop off of the load settlement curve. In each case of failure of a footing of definite diameter on dense sand, there was found a consistent ratio between the amount of settlement just before failure and the footing diameter. In the case of the one inch diameter footing the settlement prior to failure was 0.076 and 0.082 inches or roughly eight per cent of the base width. In the case of the two inch footing the settlement was 0.12 inches or six per cent of the base width, and for the three inch footing the settlement was 0.222 and 0.205 inches or 6.8 per cent. From the load settlement curves in compacted sand, a clearly marked passage into failure is evident. This failure occurred by rupture as defined by the Prandtl Theory or as described by Terzaghi for general shear failure. Therefore, in dense sands the failure load is not difficult to define. The settlement needed to produce failure was found to be between six and eight per cent of the base diameter for these tests.

Surface Tests in Medium Dense Sand.--In the case of medium dense sand the failure load was not as obvious as in the dense sand. The failure occurred in the following manner. Each increment of load produced a larger settlement than in the dense condition, but the settlement remained proportional to the load until the total settlement reached the range of about six to eight per cent of the base width. At this point the load settlement curves in each case take on a steeper slope. This is shown in Figs. 3, 4, and 5. Upon continuing the loading in some tests, another

failure seems to occur and the settlement again increases. A rupture zone can usually be seen on the surface of the sand as was evident in the dense conditions.

Surface Tests in Loose Sand.--In the failure of foundations on loose sand there was no evidence of any rupture zones on the surface. The only disturbance of the surface was due to the settlement of the foundation which left a hole in the surface slightly greater than its diameter. The exact load producing failure in the tests involving loose sand was not easily determined. The amount of settlement increased as the load grew larger; this is well illustrated in load settlement curves for the loose conditions, Figs. 3, 4, and 5, which do not show any evident of a well defined drop corresponding to any particular load.

Rupture Patterns for Surface Tests.--Although it was not the purpose of this research to study the rupture pattern, some remarks on the condition of the surface of the sand after failure occurred may be of interest. In the case of the one inch footing on a dense sand, the rupture surface was visible on the surface of the sand in the form of an egg shaped bulge on only one side of the footing. The maximum diameter of the bulge was 4.8 inches. The rupture surface appeared as a depressed concentric circle eight inches in diameter around the two inch foundation on dense sand. In the second test of the two inch base the circle was not quite concentric and had a diameter of nine inches, and bulges were noted on all sides. The failure of the three inch base produced another almost concentric depressed circle 12.6 inches in diameter with bulges



appearing just beyond the extremities of the depressed base. In all the cases of medium dense sand the ruptures did not appear completely enough to be measured definitely, although there was evidence of failure on the surface of the sand. Illustrations of the rupture patterns appear in Fig. 26.

#### Interpretation of Surface Test Results

Before any values can be assigned to the ultimate bearing capacity of the sand in the various tests a failure criterion must be defined. In the case of a failure in a dense sand, the failure load is clearly defined by a sudden sinking of the footing and by the appearance of the rupture zone on the surface of the sand. This failure load corresponds to a settlement of six to eight per cent of the footing width. In the case of a failure of a medium dense sand sometimes a second failure can be observed too. The first failure occurs at about six to eight per cent of the footing width. Therefore, the failure criterion in all cases should be considered to be the load corresponding to the settlement just prior to failure in the dense state for each diameter of footing involved. With this failure criterion defined, it is possible to find the magnitude of the load which produces failure in each case by selecting the load corresponding to the failure settlement of the dense condition from each load settlement curve. These loads are recorded as  $Q$  in Table 5.

One of the goals of this research was to determine experimentally the values of the bearing capacity factor  $N_\gamma$  and express it as a function of the angle of internal friction,  $\phi$  of the sand. In Table 5, values of height of fall of the sand, angle of internal friction, unit weight

and void ratio corresponding to the failure load  $Q$  are tabulated. Re-stating equation (2):

$$p = cN_c \xi_c + qN_q \xi_q + \frac{1}{2}\gamma bN_\gamma \xi_\gamma$$

we observe that as a first approximation of  $p$  in dealing with a so-called cohesionless material supporting a foundation on the surface, the first two terms in the above equation should become zero by virtue of the fact that theoretically  $c$  and  $q$  are both equal to zero, the result being:

$$p = \frac{1}{2}\gamma bN_\gamma \xi_\gamma$$

This equation contains only one unknown  $N_\gamma$  and its value can easily be found by the equation:

$$N_\gamma = \frac{p}{\frac{1}{2}\gamma b \xi_\gamma}$$

The results of this solution, not corrected for cohesion effect, appear in the column headed " $N_\gamma$  Not Corrected" in Table 6. It is known that there is some cohesion due to the interlocking of the grains in dense sands. In order to try to compensate for the possible existence of this cohesion values of  $p$  were plotted corresponding to the same void ratio for each diameter of base in Fig. 9. A straight line proved to be the best fitting curve connecting the values of  $p$  for each void ratio concerned. For a footing on the surface with a base width equal to zero, equation (2) becomes:

$$p = cN_c \xi_c$$

If no cohesion existed, the mean curve connecting the values of  $p$  in Fig. 9 should pass through the origin when  $b$  is equal to zero. This, however, is not the case as seen in Fig. 9; all the curves intersect the  $p$  axis at increasing values of  $p$  for decreasing values of void ratio. This can only mean that when the base diameter is equal to zero the value of the  $p$  intercept for each void ratio is equal to:

$$cN_c \xi_c$$

This value, though not large, has a considerable effect on the value of  $N_\gamma$ . Therefore, to compensate for the presence of a cohesive force due to the interlocking of the grains of the sand, a correct value for  $N_\gamma$  is:

$$N_\gamma = \frac{p - cN_c \xi_c}{\frac{1}{2}\gamma b}$$

The value of  $cN_c \xi_c$  is easily obtained by selecting the  $p$  intercept for each void ratio involved, Fig. 9. The results of this correct value for  $N_\gamma$  appear in the column headed " $N_\gamma$  Corrected" in Table 5. For use later in the computations concerning the deep load tests, values of  $c_i$ , the cohesion of interlocking, were determined for each void ratio by substituting known values of  $N_c$  and  $\xi_c$  into:

$$c_i = \frac{p}{N_c \xi_c}$$

and solving for  $c_i$ . The results of this computation are presented in Fig. 10.

Fig. 11 presents " $N_\gamma$  Corrected" and " $N_\gamma$  Not Corrected" graphically as a function of the void ratio. The effect of the cohesion of interlocking can be seen in these curves. The values of " $N_\gamma$  Not Corrected" for the cohesion effect are in most cases one hundred per cent higher than the values of " $N_\gamma$  Corrected." Therefore, although the actual value of  $c_i$  was rather small, it had a very pronounced effect on  $N_\gamma$  since the sizes of the models used were small. Fig. 12 presents the ultimate goal of the load test performed in Series I, a curve showing the bearing capacity factor  $N_\gamma$  as a function of the angle of internal friction  $\phi$  of the sand used. Fig. 12 compares favorably with the experimental results of other investigators shown in Fig. 13. Therefore, a small error in  $c$  means a terrific error in  $N_\gamma$ --a shortcoming of model work in soils.

#### Results of Deep Load Tests

Tables 7 and 8 give load settlement test results for Series II tests on deep foundations. Load settlement curves corresponding to these tests are presented in Figs. 14, 15, 16, and 17.

Deep Load Tests in Dense Sand.--The failure of a deep foundation in a dense sand was similar to the failure of a surface foundation. As the load on the base was increased, the settlement produced was proportional to the load, and the load settlement curve was approximately a straight line. When the failure load was reached, the foundation settled suddenly, but no evidence of the failure appeared on the surface. Repeated tests with the sand in a dense condition showed that there exists a ratio

between the amount of settlement just prior to failure and the footing diameter used. In the two inch footing the settlement prior to failure was .73 inches, 36.5 per cent of the footing diameter. This result was much greater than the six per cent value obtained for the two inch surface load tests. The settlement prior to failure of the three inch base in the dense sand was 1.46 inches or 47.7 per cent of the footing diameter. This also was much greater than the 8.4 per cent obtained from a similar surface test. From the load settlement curves for deep foundations in dense sand, a clearly marked passage into failure is evident. It is thought that this failure occurred by rupture as defined by Meyerhof (13) with the formation of a bulb type of failure surface. Terzaghi (14) has indicated that the bearing capacity is approximately equal to that given in equation (2), using surface bearing capacity factors, with additional effects of skin friction along the foundation shaft, and the shearing stress along a vertical outer boundary of the mass of soil adjacent to the foundation. From this work Terzaghi's Theory does not appear to be valid in dense sand. This is due to the difference in the shape of the failure surface assumed, and due to the actual bulb shaped failure surface formed when the dense sand fails.

Deep Tests in Medium Dense Sand.--The failure load in a medium dense sand is not as easy to determine as in a dense sand. The failure occurred in the following manner. Each increment of load produced a larger settlement than in the dense condition, and the first portion of the load settlement curve was a flat curve instead of a straight line. When the settlement reached a value of about 34-45 per cent of the base diameter,

the curve became steeper. This is shown in Figs. 14 and 16. This type of failure was not what could be considered a general shear failure; it should rather be termed a local shear failure.

The first indication that the theoretical bearing capacity factors for deep foundations in medium dense sand were not valid came in the first deep foundation load test. This test was run on a two inch footing in medium dense sand. The failure load was estimated to be 1580 pounds and the large lever device was used in the test. When the load reached 170 pounds the footing failed. This was about the failure load that was estimated using bearing capacity factors for surface foundations. This made it necessary for a smaller lever device to be used in all tests except those in dense sand.

The actual failure load for foundations in loose sand could not be determined directly from a load test. The load settlement curves show a steady increase in steepness with no straight line portion. Here again the failure loads were closer to those estimated by using surface bearing capacity factors instead of deep bearing capacity factors.

#### Interpretation of Deep Test Results

The failure criterion in all cases of deep tests shall be considered to be the load corresponding to the settlement just prior to failure of the foundation in the dense state for each diameter of footing involved. The failure criterion is determined by the same reasoning used in the surface tests. The settlement just prior to failure of the two and three inch footings in the dense states was 0.73 and 1.46 inches respectively. This can also be expressed as 36.5 and 47.7 per cent of the respective base

diameters. The settlement of the two inch footing prior to failure was determined by extending the straight line portion of the load settlement curve until it crossed the settlement axis; this intercept was taken as zero settlement and eliminated the nonuniform settlement in the first portion of the curve shown in Fig. 15. Knowing the settlement, prior to failure in each case, makes it possible to determine the failure load from the load settlement curves of each load test. The failure loads are recorded as  $Q$  in Table 9.

The failure loads in loose and medium dense sands were less than estimated using Caquot's theoretical bearing capacity factors for deep foundations. The reason for this discrepancy is in the assumptions used in deriving these values. In deriving bearing capacity factors for deep foundations a general shear failure and rigid soil is assumed. The soil in the plastic zones, and for some distance beyond the failure surface, is actually compressed and may be subject to volume changes. This compression of the soil is particularly important when the soil is loose and compressible. A complete failure surface bulb cannot be developed; therefore, the basis on which the bearing capacity factors are derived does not actually occur in loose and medium dense sands.

The second goal of this research was to determine experimentally the values of deep bearing capacity factors and express these as a function of the angle of internal friction of the sand. The general bearing capacity equation is:

$$p = cN'_c + \gamma DN'_q + \frac{1}{2}\gamma bN'_\gamma \quad (4)$$

where:

$$N'_c = (N'_q - 1) \cot \phi$$

$$c = c_i = \text{Cohesion due to interlocking of grains}$$

Substituting the above value of  $N'_c$  into equation (4) we get:

$$p = c_i \cot \phi (N'_q - 1) + \gamma D N'_q + \frac{1}{2} \gamma b N'_\gamma \quad (5)$$

Solving equation (5) for  $N'_q$  we get:

$$N'_q = \frac{p + c_i \cot \phi - \frac{1}{2} \gamma b N'_\gamma}{c_i \cot \phi + \gamma D} \quad (6)$$

Table 9 presents a tabular solution of equation (6) for loose, medium dense, and dense sands. The effect of  $N'_\gamma$  on  $N'_q$  can be estimated by considering the base to be equal to zero, giving:

$$N'_q = \frac{p + c_i \cot \phi}{c_i \cot \phi + \gamma D} \quad (7)$$

Table 9 also presents a tabular solution of equation (7). The values of  $c_i$  used in the computations were determined from Fig. 10.  $N'_q$  values obtained from equation (6) do not differ greatly from values obtained from equation (7). Therefore, the effect of  $N'_\gamma$  can be neglected when small footings are used and the final values of  $N'_q$  used are determined from equation (7). Fig. 18 presents the ultimate goal of Series II,



a curve showing the bearing capacity factor  $N'_q$  as a function of the angle of internal friction  $\phi$ , of the sand. Values of  $N'_c$  can be obtained from the relation:

$$N'_c = (N'_q - 1) \cot \phi$$

From Fig. 18 it becomes apparent that the bearing capacity factor  $N'_q$  is approximately equal to  $N_q$  for surface foundations for loose and medium dense sands, and approaches the theoretical value of  $N_q$  for dense sands. Therefore, it would be wise to use  $N'_q$  equal to  $N_q$  for design purposes except when the sand is very dense.

## CHAPTER VI

## CONCLUSIONS

The following conclusions can be drawn from the results of this research. Conclusions one through four deal with surface tests, and five through nine deal with deep tests. It should be kept in mind that the deep tests apply only to point bearing capacity.

1. The observed bearing capacity for surface foundations in sand agrees reasonably well with the theory.

2. Three types of rupture exist in sand: general shear failure, local shear failure, and punching. These three types occur in dense, medium dense, and loose sands respectively.

3. Failure occurs in surface foundations when the settlement of the base reaches six to eight per cent of the footing diameter.

4. A cohesion due to grain interlocking is apparent in sand, and affects the value of bearing capacity observed especially in small model tests.

5. The observed bearing capacity of deep foundations in sand is considerably less than estimated by the present theory because of the compressibility of the sand. It is believed that the failure surfaces assumed in the theory do not develop in loose and medium dense sands.

6. Three types of failure also appear to exist in the deep load tests in sand. In dense sand general shear failure occurs; in medium dense sand local shear failure occurs; and in loose sand, because of

the compressibility of the sand, the footing fails by punching farther and farther into the sand.

7. Failure occurs in deep foundations when the settlement of the foundation reaches thirty-five to fifty per cent of the footing diameter.

8. Use of theoretical values of bearing capacity factors derived for deep foundations in loose and medium dense sand will lead to over-estimating the point bearing capacity of the footing concerned.

9. Close approximation of the ultimate bearing capacity of foundations in loose and medium dense sand can be obtained by using bearing capacity factors derived from surface and shallow foundation tests or theoretical surface bearing capacity factors.

## CHAPTER VII

### RECOMMENDATIONS

In order to aid the theoretical determination of more accurate values of bearing capacity factors for deep foundations, it is recommended that studies be made to determine the shape of the failure surface for loose, medium dense, and dense sand. This could probably be done in a similar manner to that used by DeBeer and Vesic (15). The sand used in the tests should consist of two portions, one portion a dark color and the other portion a light color. The sand should be mixed with cement in proportions of ten to one so that the angle of internal friction of the mixture would not be different from that of the sand by itself. The sand should be stored in two charging containers so that alternate one-half inch layers of light and dark sand could be placed in the test bin. The desired density of the sand could be obtained by dropping the sand from various heights. Each layer of the sand should be struck off level by a very sharp cutting device. This would probably be the most difficult part of the test since the pipe containing the loading rod would be in the center of the test bin. Load tests could be run similar to those described in this project. After failure of the footing water should be allowed to seep into the test bin to hydrate the cement. After a few days the hardened sample should be sawed across the footing and the shape of the failure surface photographed.

The tests recommended above need further study rather than further study of load tests, because it has been shown in the research conducted in this project that the failure surfaces assumed for theoretical analysis of the bearing capacity factors did not develop in the tests on loose and medium dense sand. With a better understanding of the failure surfaces of loose and medium dense sand, it might be possible to develop the theory concerning deep foundations to the extent that shallow and surface bearing capacity theory has been developed.

Load tests could also be performed on piles placed and driven into the sand and the effect of skin friction and the method of installation studied.

In addition to the above recommendations, this author further suggests that various shapes of footings should be studied by load testing.

## APPENDIX

Table 1. Glossary of Abbreviations

$A$	= area
$b$	= diameter of footing
$c$	= cohesion
$c_i$	= cohesion due to interlocking of sand grains
$D$	= depth of foundation
$e$	= void ratio--volume of voids per unit volume of solid soil constituents
$G_s$	= specific gravity of soil solids
$h$	= height of fall of the sand
$K_p$	= coefficient of passive earth pressure
$N_c, N_q, N_\gamma$	= bearing capacity factors for surface foundations
$N'_c, N'_q, N'_\gamma$	= bearing capacity factors for deep foundations
$p$	= pressure per unit of area
$Q$	= total load at failure on the point
$Q_s$	= total load at failure on sides (skin friction)
$q$	= surcharge = $\gamma D$
$s$	= settlement of foundation
$\gamma$	= unit weight of the sand
$\phi$	= angle of internal friction
$\xi_c, \xi_q, \xi_\gamma$	= shape factors
$\eta$	= angle describing the extend of the Rankine zone

Table 2. Load Settlement Test Results Series I Footings on the Surface

Group 1 ( $e = 1.07$ )

Load (grams)	1" Base Settlement (inches)		Load (grams)	2" Base Settlement (inches)		Load (pounds)	3" Base Settlement (inches)	
	Test 1	Test 2		Test 1	Test 2		Test 1	Test 2
41.6	0.002	0.002	267.5	0.000	0.000	1.37	0.000	0.000
91.6	0.005	0.007	728.4	0.020	0.018	2.38	0.005	0.004
141.6	0.012	0.009	1202.7	0.066	0.060	3.38	0.020	0.020
191.6	0.031	0.025	1402.7	0.095	0.090	4.64	0.049	0.045
241.6	0.042	0.035	1602.7	0.120	0.110	5.89	0.082	0.084
291.6	0.064	0.055	2070.7	0.190	0.200	7.13	0.110	0.100
341.6	0.094	0.095	2528.3	0.252	0.270	8.40	0.148	0.150
391.6	0.123	0.121	2984.1	0.377	0.400	9.63	0.182	0.175
491.6	0.203	0.22				10.65	0.215	0.214
541.6	0.234	0.241				11.68	0.247	0.246
591.6	0.286	0.288				12.28	0.285	0.274
691.6	0.386	0.394				13.81	0.318	0.322
						14.70	0.340	0.335
						16.69	0.425	0.410
						18.70	0.504	0.480



Table 3. Load Settlement Test Results Series I Footings on the Surface

Group 2 ( $e = 0.92$ )

Load (grams)	1" Base Settlement (inches)		Load (grams)	2" Base Settlement (inches)		Load (pounds)	3" Base Settlement (inches)	
	Test 1	Test 2		Test 1	Test 2		Test 1	Test 2
41.6	0.000	0.000	267.5	0.000	0.000	1.37	0.000	0.000
241.6	0.008	0.005	741.8	0.002	0.002	4.21	0.005	0.003
341.6	0.029	0.021	1209.0	0.012	0.010	9.21	0.040	0.035
541.6	0.072	0.050	1664.8	0.030	0.025	14.21	0.107	0.120
641.6	0.102	0.090	2125.7	0.045	0.050	19.21	0.165	0.160
841.6	0.180	0.160	2692.1	0.060	0.060	24.21	0.235	0.215
1041.6	0.280	0.260	3262.0	0.068	0.081	29.21	0.364	0.340
			3827.4	0.020	0.125	34.21	0.443	0.420
			4391.3	0.182	0.200	39.21	0.565	0.520
			4956.6	0.196	0.220			
			5414.2	0.234	0.260			
			5914.2	0.300	0.320			

Table 4. Load Settlement Test Results Series I Footings on the Surface

Group 3 ( $e = 0.86$ )

Load (grams)	1" Base Settlement (inches)		Load (grams)	2" Base Settlement (inches)		Load (pounds)	3" Base Settlement (inches)	
	Test 1	Test 2		Test 1	Test 2		Test 1	Test 2
41.6	0.002	0.000	267.5	0.000	0.000	1.37	0.000	0.000
241.6	0.009	0.010	2537.5	0.034	0.033	4.21	0.002	0.003
441.6	0.025	0.021	3101.4	0.045	0.050	9.21	0.015	0.010
541.6	0.035	0.030	3562.3	0.055	0.060	14.21	0.039	0.020
741.6	0.055	0.040	4019.9	0.066	0.070	21.21	0.100	0.080
941.6	0.085	0.080	4487.9	0.080	0.080	24.21	0.117	0.100
1041.6	0.100	0.090	4962.2	0.103	0.090	34.21	0.170	0.150
1166.6	0.166	0.180	5527.6	0.115	0.100	39.21	0.213	0.190
1291.6	0.242	0.250	6094.0	0.135	0.120	44.21	0.270	0.269
			6663.9	0.166	0.160	49.21	0.325	0.340
			7119.7	0.191	0.200	54.21	0.415	0.420
			7685.0	0.220	0.230			
			9955.0	0.522	0.500			

Table 5. Load Settlement Test Results Series I Footings on the Surface

Group 4 ( $e = 0.73$ )

Load (grams)	1" Base Settlement (inches)		Load (pounds)	2" Base Settlement (inches)		Load (pounds)	3" Base Settlement (inches)	
	Test 1	Test 2		Test 1	Test 2		Test 1	Test 2
41.6	0.000		0.60	0.000	0.000	1.4	0.000	0.000
499.2	0.002		3.45	0.003	0.000	4.2	0.000	0.000
973.5	0.006		13.45	0.013	0.019	14.2		0.005
1429.3	0.008		18.45	0.023		24.2		0.019
1890.2	0.015		23.45	0.033	0.039	26.2	0.010	
2455.5	0.030		28.45	0.042		34.2		0.028
3025.5	0.047		33.45	0.052	0.059	44.2		0.037
3592.0	0.082		38.45	0.065		51.2	0.025	
4157.4	0.290		43.45	0.077	0.088	54.2		0.047
			48.45	0.095	0.113	64.2		0.051
			53.45	0.120	0.142	72.2	0.040	
			58.45	Failure	Failure	74.4		0.058
						82.2	0.049	
						84.2		0.070
						92.2	0.058	
						94.2		0.080
						102.2	0.065	
						104.2		0.090

Table 5 (Continued)

Load (grams)	1" Base Settlement (inches)		Load (pounds)	2" Base Settlement (inches)		Load (pounds)	3" Base Settlement (inches)	
	Test 1	Test 2		Test 1	Test 2		Test 1	Test 2
						112.2	0.079	
						114.2		0.100
						117.2	0.085	
						122.2	0.091	
						124.2		0.120
						127.2	0.100	
						132.2	0.110	
						134.2		0.132
						137.2	0.121	
						142.2	0.139	
						144.2		0.160
						152.2	0.185	
						154.2		0.181
						162.2	0.222	
						164.2		0.205
						167.2	0.722	Failure

Table 6. Tabular Computation of  $N_\gamma$

h (in)	$\phi$	$\gamma$ lb/ft <sup>3</sup>	e	Q	p=Q/A lb/ft <sup>2</sup>	$cN_c \xi_c$ lb/ft <sup>2</sup>	$\frac{1}{2}\gamma b \xi_\gamma$ lb/ft <sup>2</sup>	$N_\gamma$ Corrected	$N_\gamma$ Not Corrected
1" Footing									
0	31.0	80.0	1.07	330.0g	133.2	85	2.33	20.7	57.1
0	31.0	80.0	1.07	337.0g	136.4	85	2.33	22.0	58.6
8	35.0	86.5	0.92	575.0g	233.0	120	2.52	45.0	92.0
8	35.0	86.5	0.92	606.0g	246.0	120	2.52	50.0	97.7
16	38.0	90.0	0.843	1060.0g	428.0	200	2.62	87.0	163.0
16	37.5	89.4	0.86	1060.0g	428.0	200	2.61	87.4	164.0
	43.0	96.0	0.73	3800.0g	1540.0	920	2.80	222.0	550.0
	43.0	96.0	0.73	3660.0g	1480.0	920	2.80	200.0	530.0
2" Footing									
0	31.0	80.0	1.07	1600.0g	162.0	85	4.67	16.5	34.8
0	31.0	80.0	1.07	1620.0g	163.4	85	4.67	17.0	35.0
8	35.0	86.5	0.92	3830.0g	387.0	120	5.05	52.8	76.6
8	35.0	86.5	0.92	3830.0g	387.0	120	5.05	52.8	76.6
16	37.5	89.4	0.86	5650.0g	571.0	200	5.22	71.2	109.5
16	37.5	89.4	0.86	6100.0g	616.0	200	5.22	80.0	117.0
	43.0	96.0	0.73	55.01b	2520.0	920	5.60	286.0	450.0
	43.0	96.0	0.73	53.01b	2430.0	920	5.60	270.0	434.0

Table 6 (Continued)

h	$\phi$	$\gamma$	e	Q	p=Q/A	$cN_c \xi_c$	$\frac{1}{2} \gamma b \xi_\gamma$	$N_\gamma$	$N_\gamma$ Not
(in)		lb/ft <sup>3</sup>			lb/ft <sup>2</sup>	lb/ft <sup>2</sup>	lb/ft <sup>2</sup>	Corrected	Corrected
3" Footing									
0	31.0	80.0	1.07	4750.0g	213.0	85	7.00	18.3	30.4
0	31.0	80.0	1.07	4700.0g	211.0	85	7.00	18.0	30.2
8	35.0	86.5	0.92	22.7lb	463.0	120	7.57	45.4	61.0
8	35.0	86.5	0.92	23.0lb	468.0	120	7.57	46.0	61.8
16	37.5	89.4	0.86	39.3lb	800.0	200	7.82	76.8	102.0
16	37.5	89.4	0.86	40.0lb	824.0	200	7.82	79.8	105.0
	43.0	96.0	0.73	163.0lb	3320.0	920	8.41	285.0	395.0
	43.0	96.0	0.73	168.0lb	3420.0	920	8.41	297.0	406.0

Table 7. Load Settlement Test Results Series II Footings Deep

Group 1 (e = 1.07)				Group 2 (e = 0.92)				
2" Base		3" Base		2" Base		3" Base		
Load	Settlement	Load	Settlement	Load	Settlement	Load Settlement		
(pounds)	(inches)	(pounds)	(inches)	(pounds)	(inches)	(pounds)	(inches)	(inches)
					Test 1	Test 2		
0	0.000	0	0.000	29	0.015	0.060	44	0.045
		22	0.000					
29	0.050	44	0.000	49	0.105	0.077	84	0.060
37	0.058	64	0.000	69	0.227	0.160	124	0.100
57	0.106	84	0.015	79	0.360	0.190	164	0.190
77	0.490	104	0.034	87	0.475	0.200	204	0.381
85	0.696	124	0.061	97	0.640	0.230	224	0.500
93	2.50	144	0.105	105	0.807		244	0.640
		164	0.165	107		0.718	264	0.820
		204	0.505	113	0.985		284	1.045
		224	0.665	115		0.852	304	1.272
		244	0.915	113	1.510		324	1.495
		264	1.240	135		2.90	344	1.755
		284	1.675	153	2.20		364	2.020
		304	1.940	173	4.00		384	2.300
		324	2.335				404	2.632
		364	3.250				424	2.970
							464	4.5+

Table 8. Load Settlement Test Results Series II Footings Deep

Group 3 (e = 0.86)				Group 4 (e = 0.73)					
2" Base		3" Base		2" Base		2" Base		3" Base	
Load (pounds)	Settlement (inches)	Load (pounds)	Settlement (inches)	Load (pounds)	Settlement (inches)	Load (pounds)	Settlement (inches)	Load (pounds)	Settlement (inches)
0	0.000	44	0.000	0	0.000	0	0.000	0	0.000
29	0.052	84	0.001	35	0.010	90	0.000	100	0.000
49	0.071	124	0.010	90	0.035	190	0.010	354	.015
69	0.110	164	0.029	140	0.380	290	.074	610	.039
89	0.184	204	0.074	165	0.118	390	.100	855	.065
109	0.292	244	0.135	180	0.130	490	.128	1122	.089
129	0.475	284	0.270	230	0.154	590	.146	1367	.114
149	0.845	324	0.385	280	0.170	690	.164	1524	.146
157	1.010	364	0.535	330	0.185	790	.184	1744	.208
165	1.305	404	0.745	380	0.198	890	.200	2000	.254
185	2.375	444	1.095	430	0.211	1140	.264	2238	.288
205	3.125	484	1.490	480	0.226	1394	.345	2488	.325
225	4.30	524	1.980	530	0.241	1494	.365	2745	.370
		564	2.440	580	0.255	1594	.409	2995	.433
		604	2.90	630	0.270	1694	.460	3359	.580
		644	3.520	680	0.282	1794	.495	3609	.590
		684	4.430	780	0.312	1894	.560	3859	.600
				880	0.347	1994	.620	4109	.620
				980	0.378	2094	.700	4319	.640
				1080	0.412	2194	.780	4582	.650
				1180	0.453	2294	.860	5102	.680
				1280	0.500	2394	.955	5357	.700
				1380	0.550	2494	1.035	5612	.735
				1480	0.615	2594	1.125	6096	.820
				1580	0.690	2694	1.245	6367	.875
				1680	0.780	2794	1.307	6580	.910
				1780	0.822	2894	1.560	6840	.960
				1880	1.24	2994	1.650	7096	1.040



Table 8 (Continued)

Group 3 ( $e = 0.86$ )				Group 4 ( $e = 0.73$ )					
2" Base		3" Base		2" Base		2" Base		3" Base	
Load	Settlement	Load	Settlement	Load	Settlement	Load	Settlement	Load	Settlement
(pounds)	(inches)	(pounds)	(inches)	(pounds)	(inches)	(pounds)	(inches)	(pounds)	(inches)
				1980	1.39	3250	2.310	7366	1.115
				2080	1.56	3495	3.130	7629	1.170
				2180	1.72	3645	3.700	7888	1.220
				2280	1.90			8156	1.300
								8646	1.470
								8908	2.10

Table 9. Tabular Computation of  $N'_q$

	$\phi$	$\cot \phi$	$\gamma$ lb/ft <sup>3</sup>	$q$ lb/ft <sup>2</sup>	$p$ lb/ft <sup>2</sup>	$N_\gamma$	$c$ lb/ft <sup>2</sup>	$\frac{1}{2}\gamma b N_\gamma$ lb/ft <sup>2</sup>	$c \cot \phi$ lb/ft <sup>2</sup>	(c) $p+c \cot \phi$ lb/ft <sup>2</sup>	(a) $p+c \cot \phi - \frac{1}{2}\gamma b N_\gamma$ lb/ft <sup>2</sup>	(b) $c \cot \phi + \gamma D$ lb/ft <sup>2</sup>	$N'_q = \frac{(a)}{(b)}$ (eq. 6)	$N'_q = \frac{(c)}{(b)}$ (eq. 7)
2 in Plate	31°	1.73	80.0	86	3940	20	2.13	133	3.68	3944	3810	204	18.7	19.4
	35°	1.43	86.5	108	4960	45	2.17	324	3.10	4963	4639	219	21.7	22.6
	35°	1.43	86.5	102	4680	45	2.17	324	3.10	4683	4359	219	19.9	21.4
	37.5°	1.30	89.4	144	6600	75	2.75	558	3.57	6604	6046	232	26.2	28.6
	43°	1.07	96.0	1880	86400	250	6.96	2000	7.45	86408	84408	248	341.0	349.0
	43°	1.07	96.0	2250	103100	250	6.96	2000	7.45	103108	101108	248	409.0	417.0
3 in Plate	31°	1.73	80.0	276	5620	20	2.13	200	3.68	5624	5424	304	17.9	18.5
	35°	1.43	86.5	320	6520	45	2.17	486	3.10	6523	6037	327	18.4	19.9
	37.5°	1.30	89.4	480	9770	75	2.75	838	3.57	9774	8936	339	26.4	28.8
	43°	1.07	96.0	8466	173000	250	6.96	3000	7.45	173008	170008	368	463.0	471.0
	43°	1.07	96.0	8646	176000	250	6.96	3000	7.45	176008	173008	368	471.0	479.0

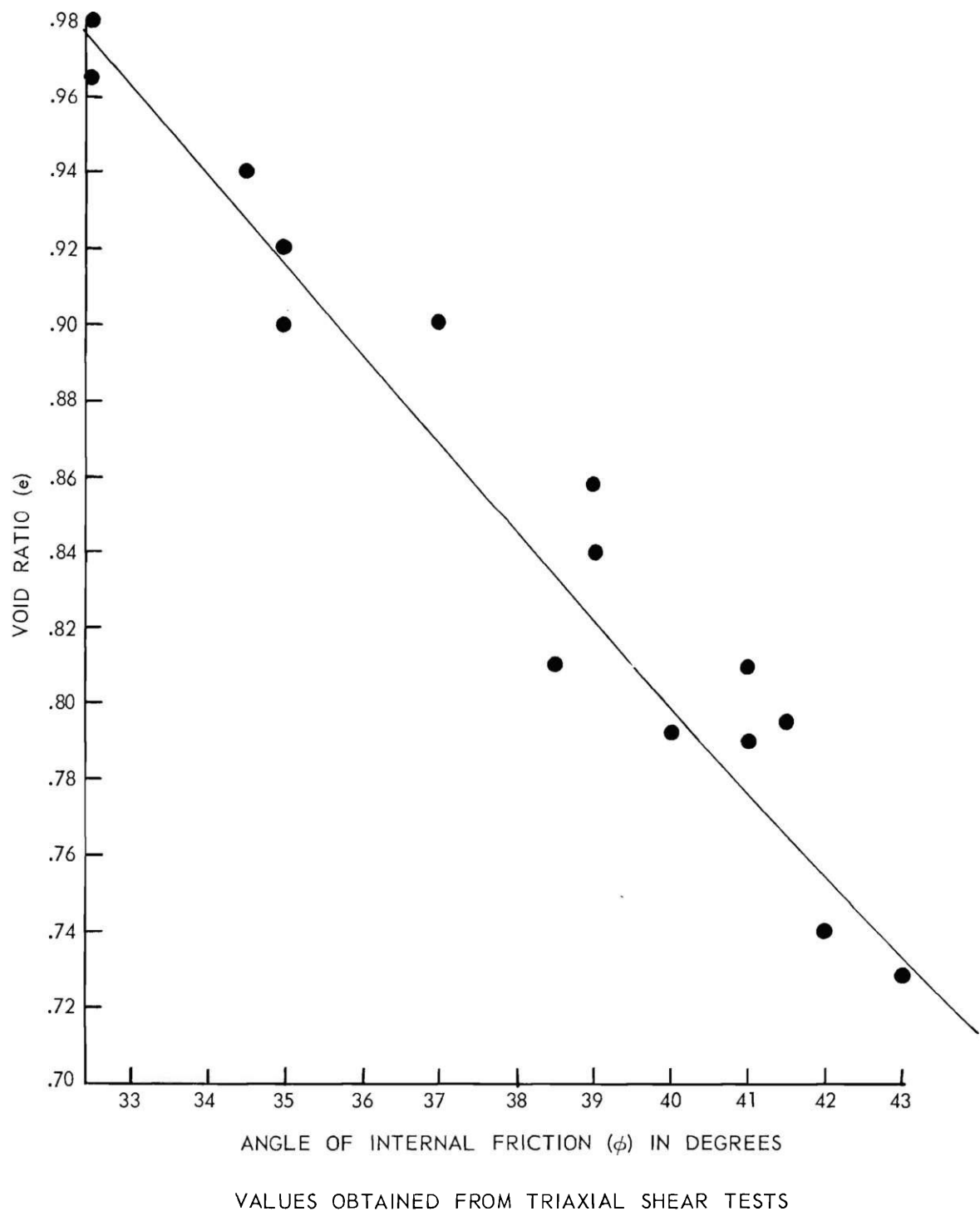


Figure 1. Angle of Internal Friction vs Void Ratio.

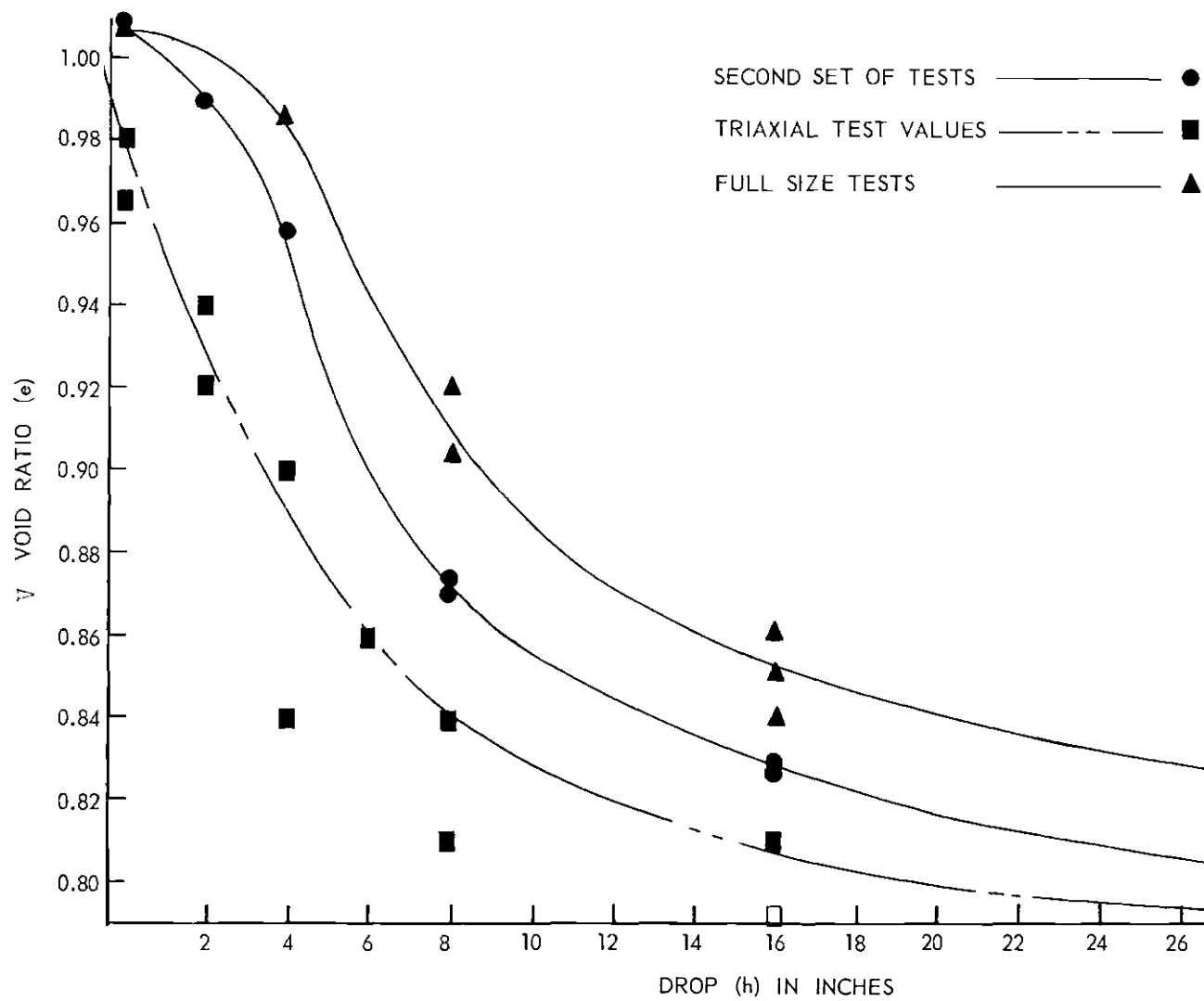


Figure 2. Height of Fall vs Void Ratio Curves.

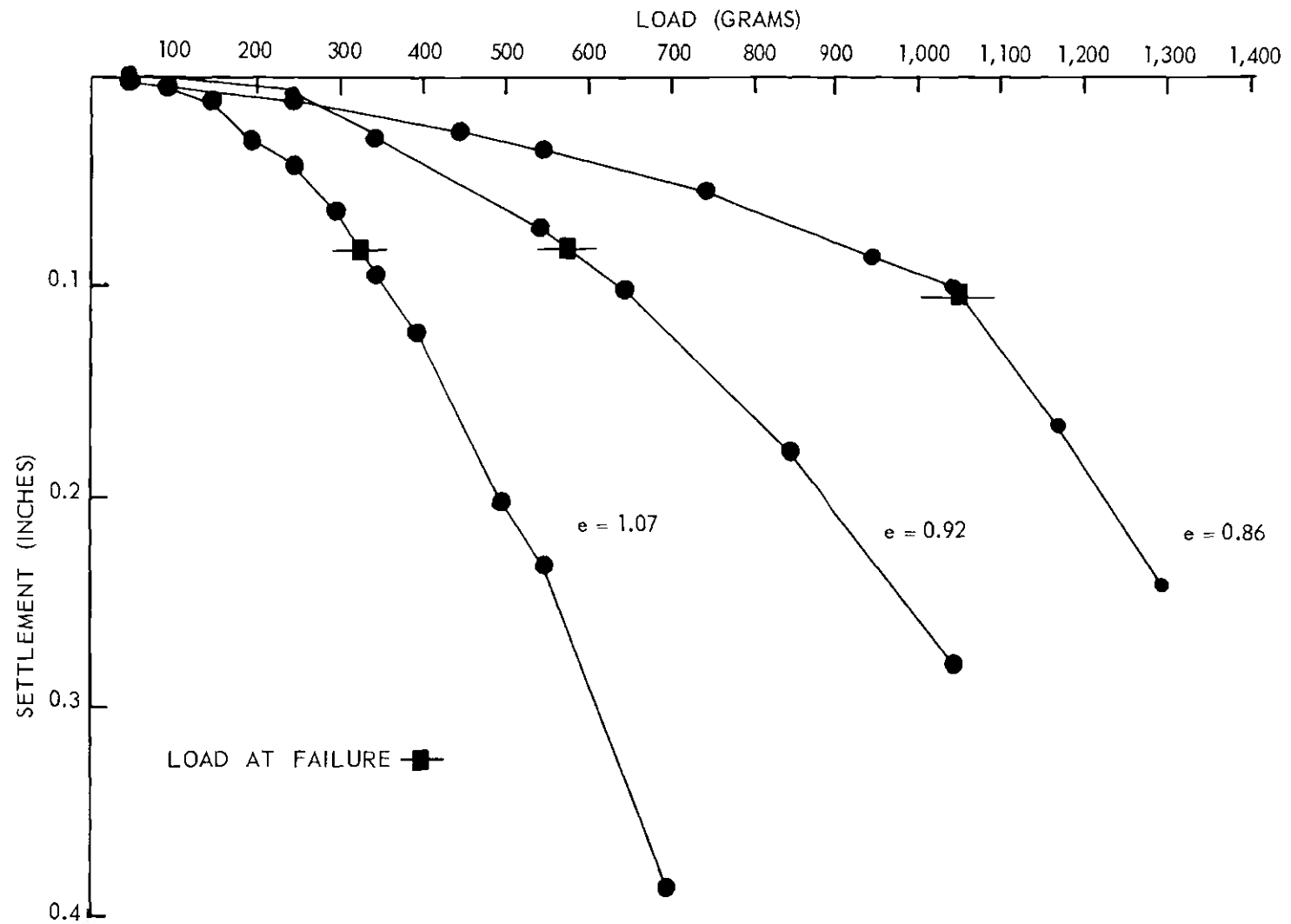


Figure 3. Load Settlement Curves (1" Footings).

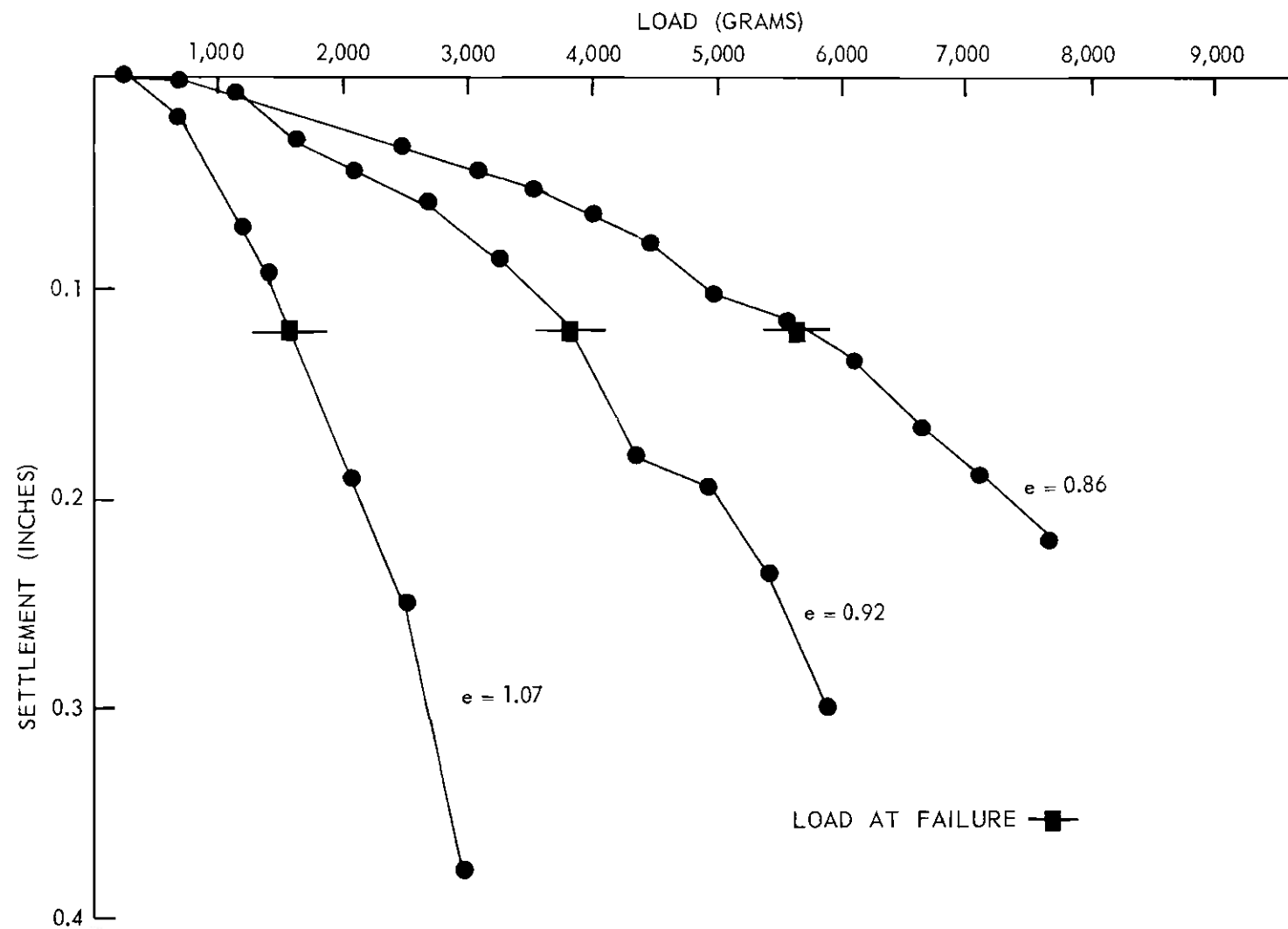


Figure 4. Load Settlement Curves (2" Footings).

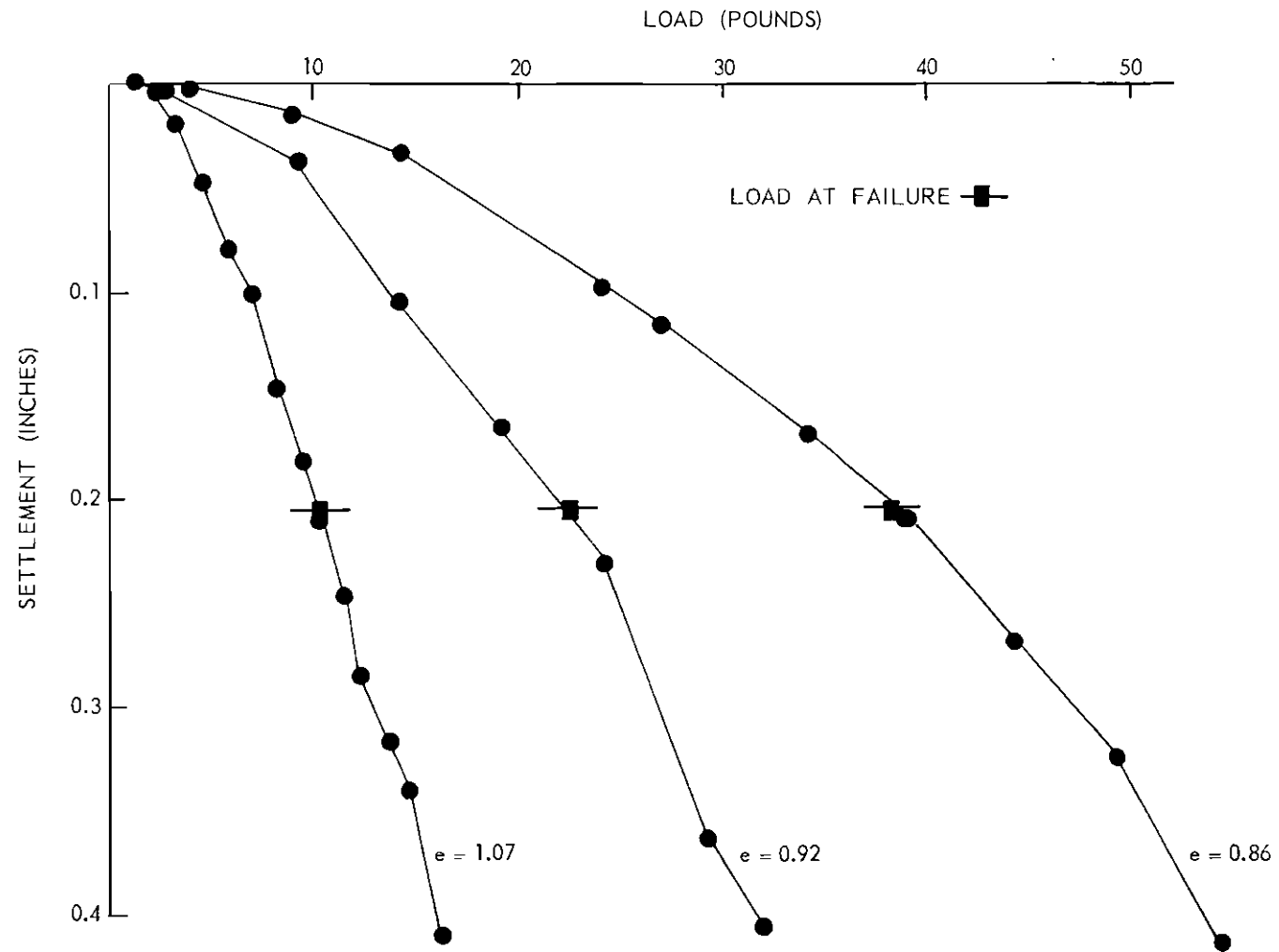


Figure 5. Load Settlement Curves (3" Footings).

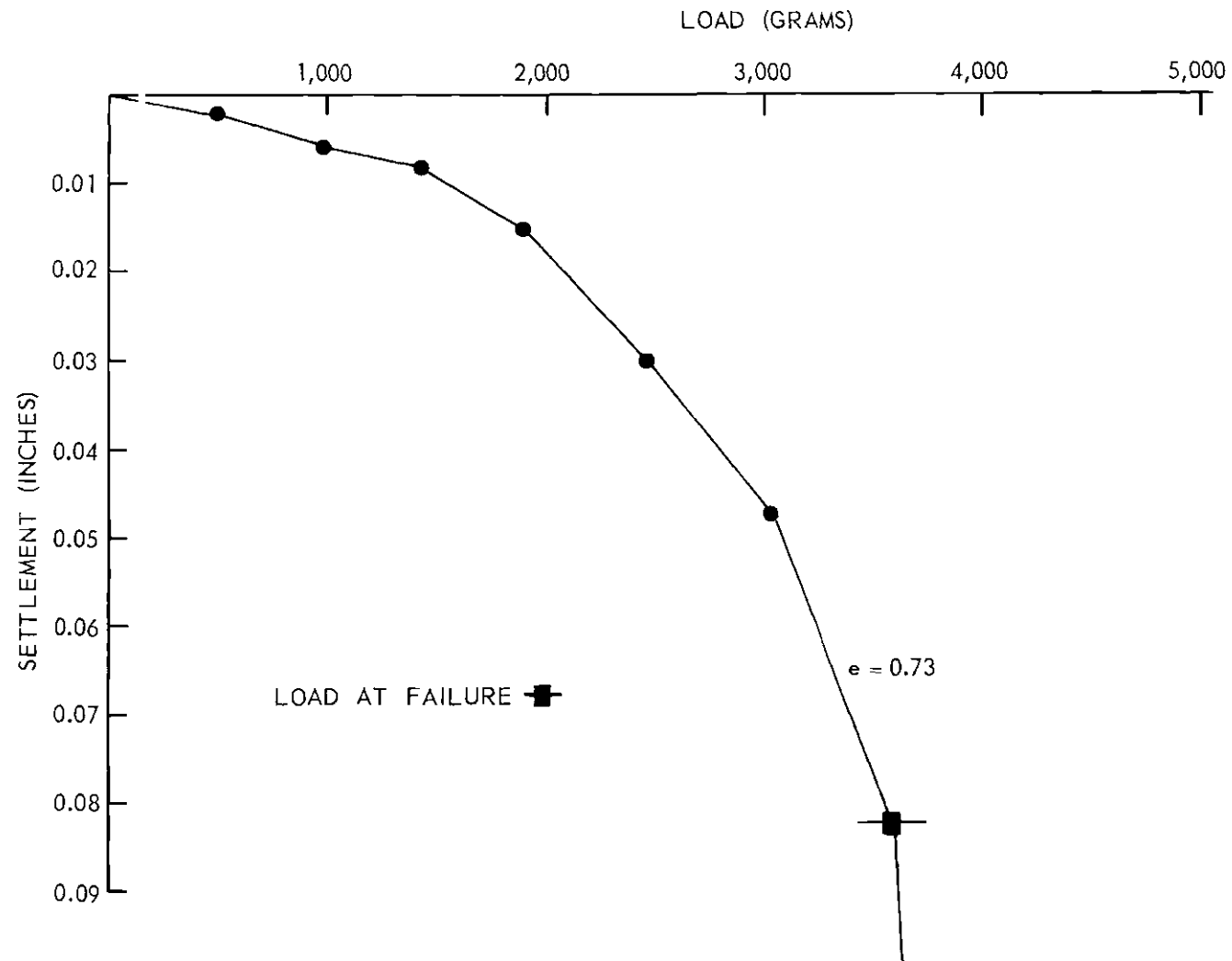


Figure 6. Load Settlement Curve (1" Footing).



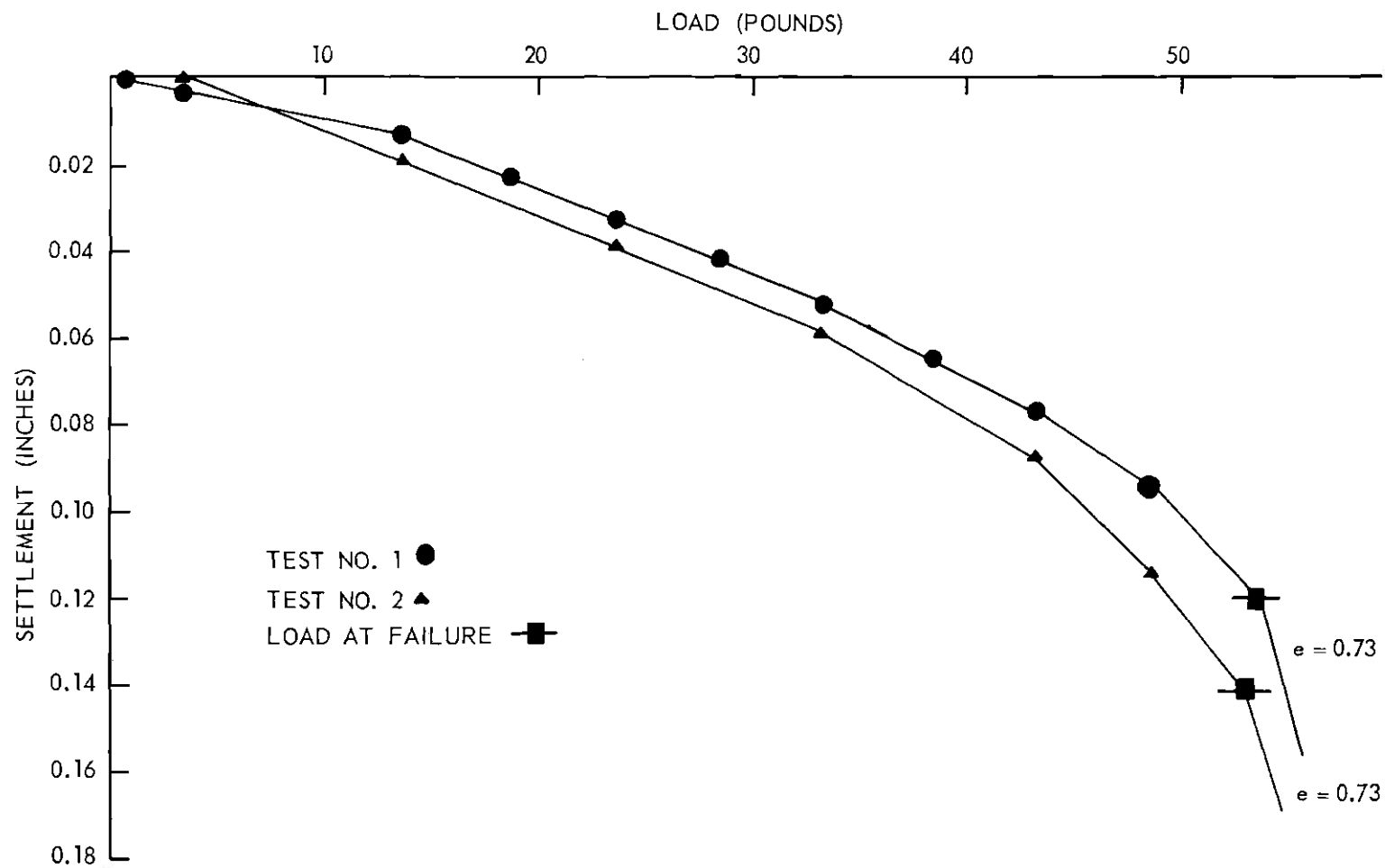


Figure 7. Load Settlement Curves (2" Footings).

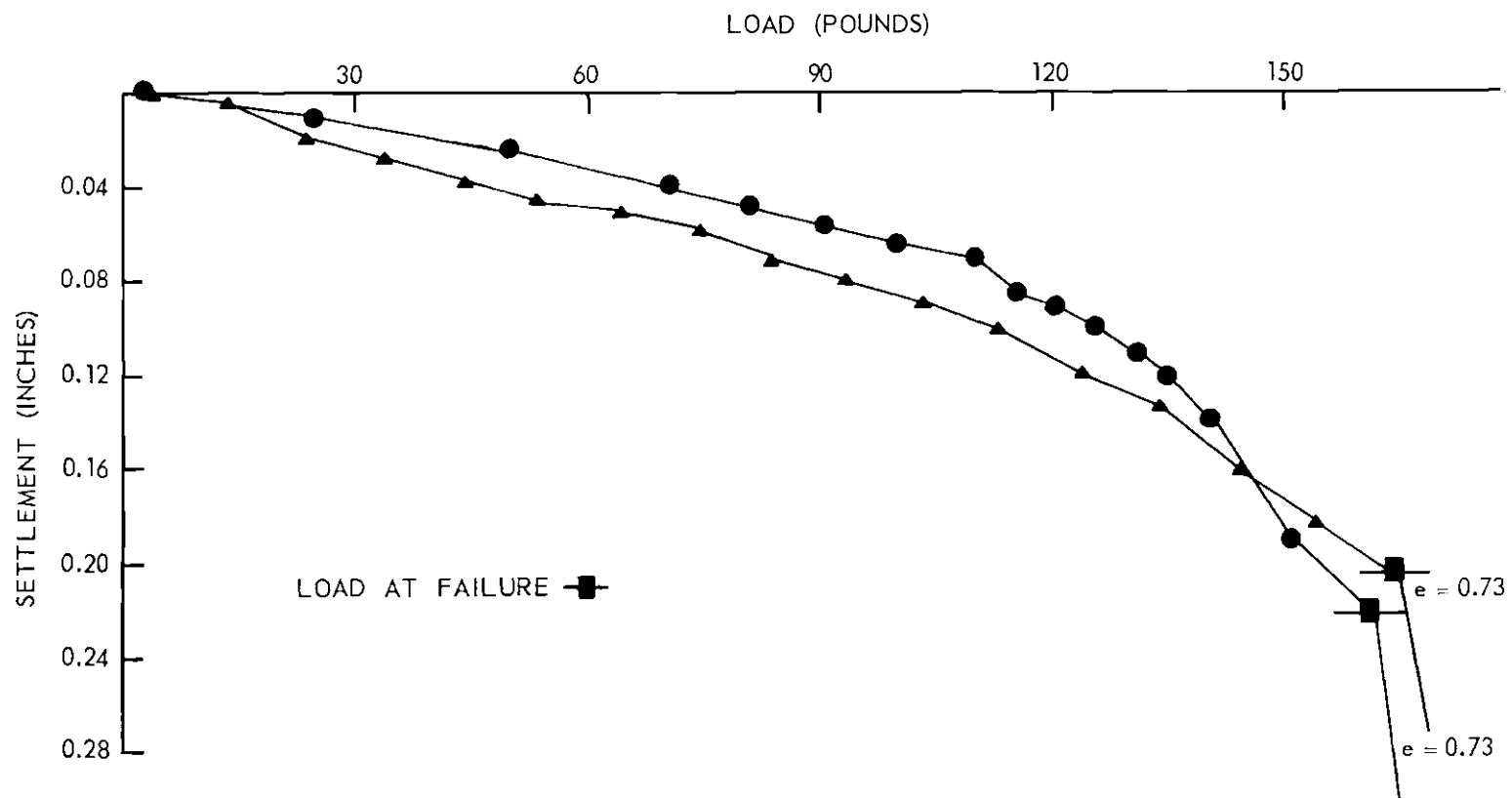


Figure 8. Load Settlement Curves (3" Footings).

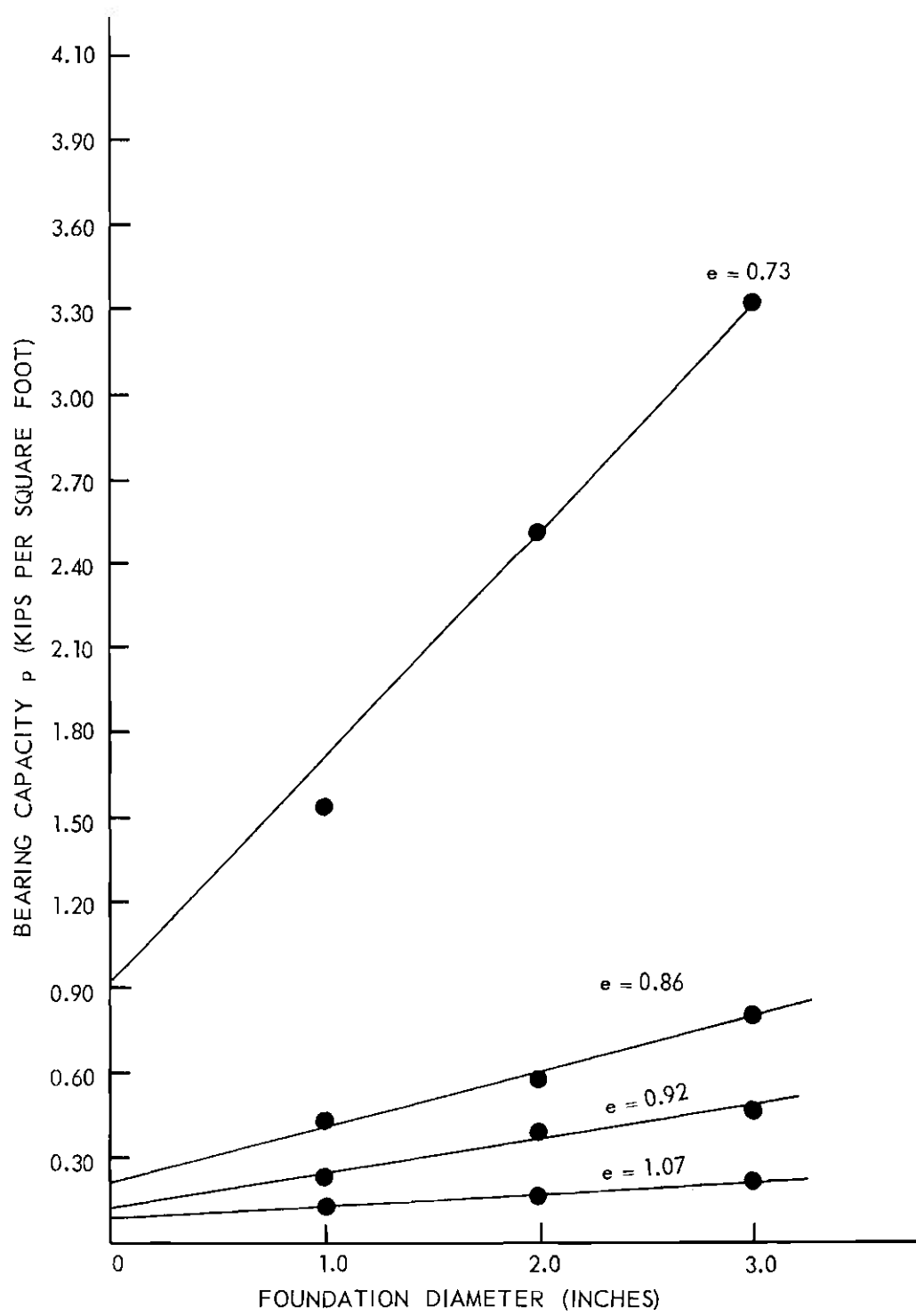


Figure 9. Graph Showing Existence of Cohesion in the Sand.

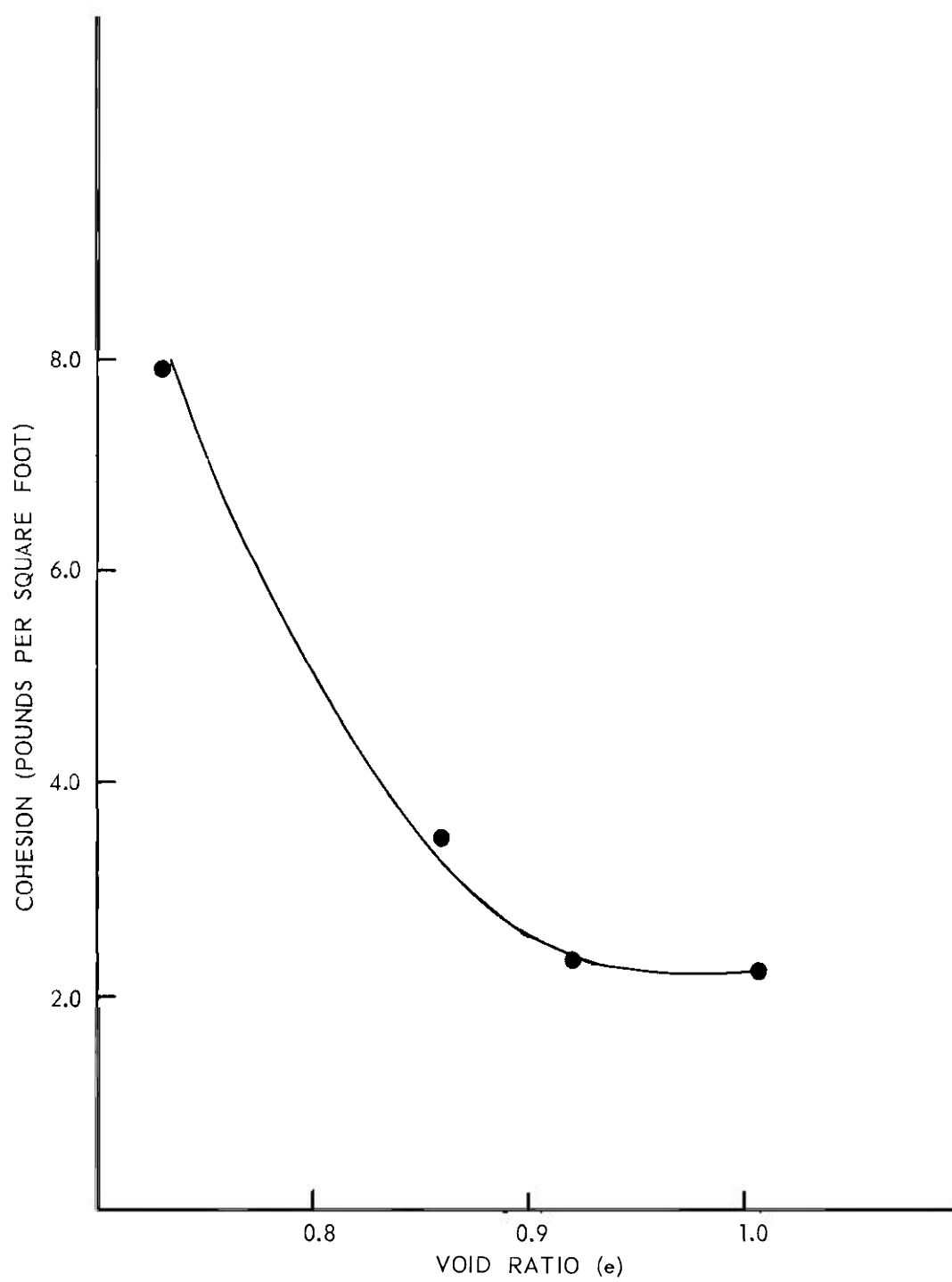


Figure 10. Void Ratio vs Cohesion Curve.

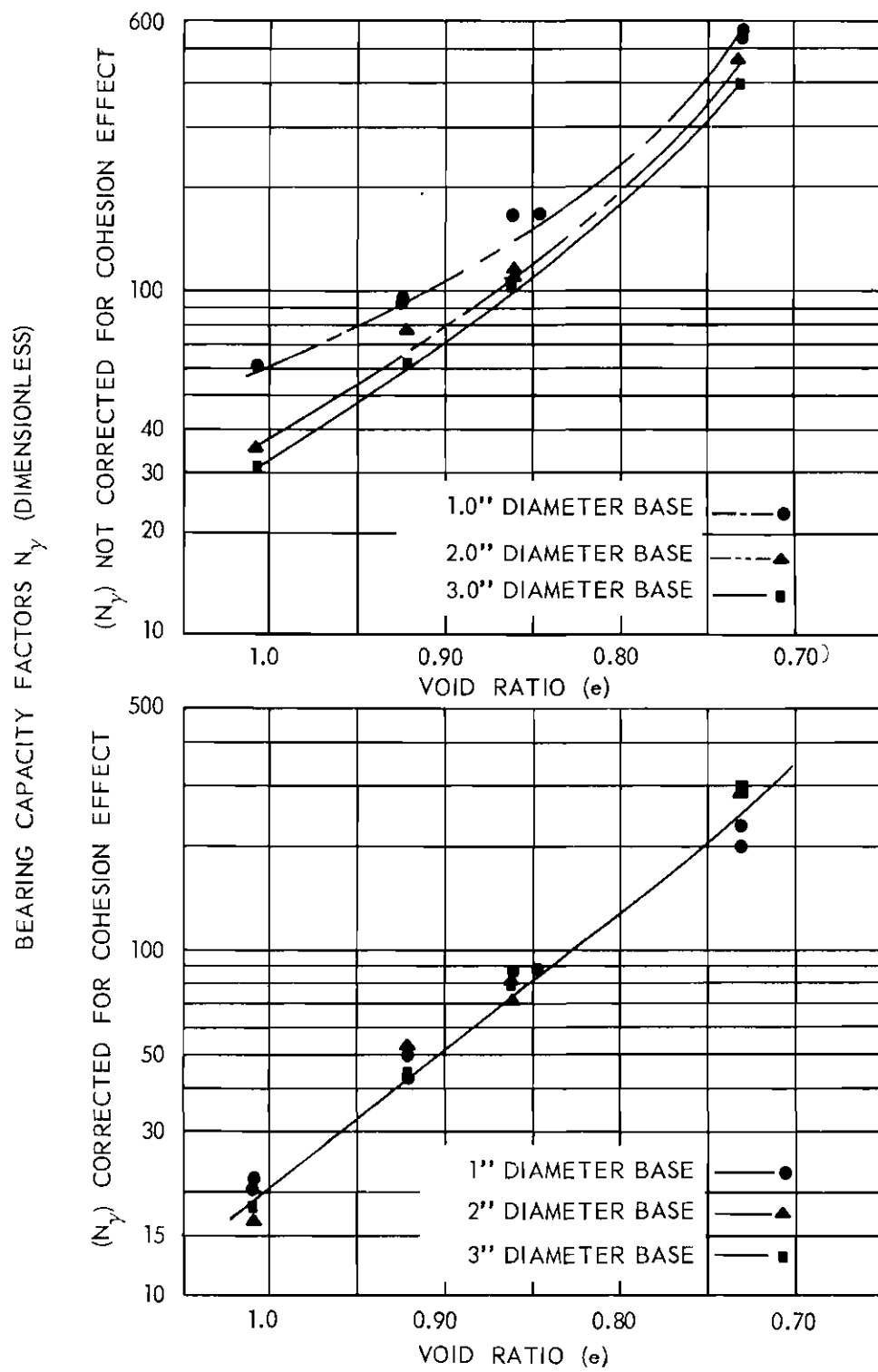


Figure 11. Bearing Capacity Factors vs Void Ratio.

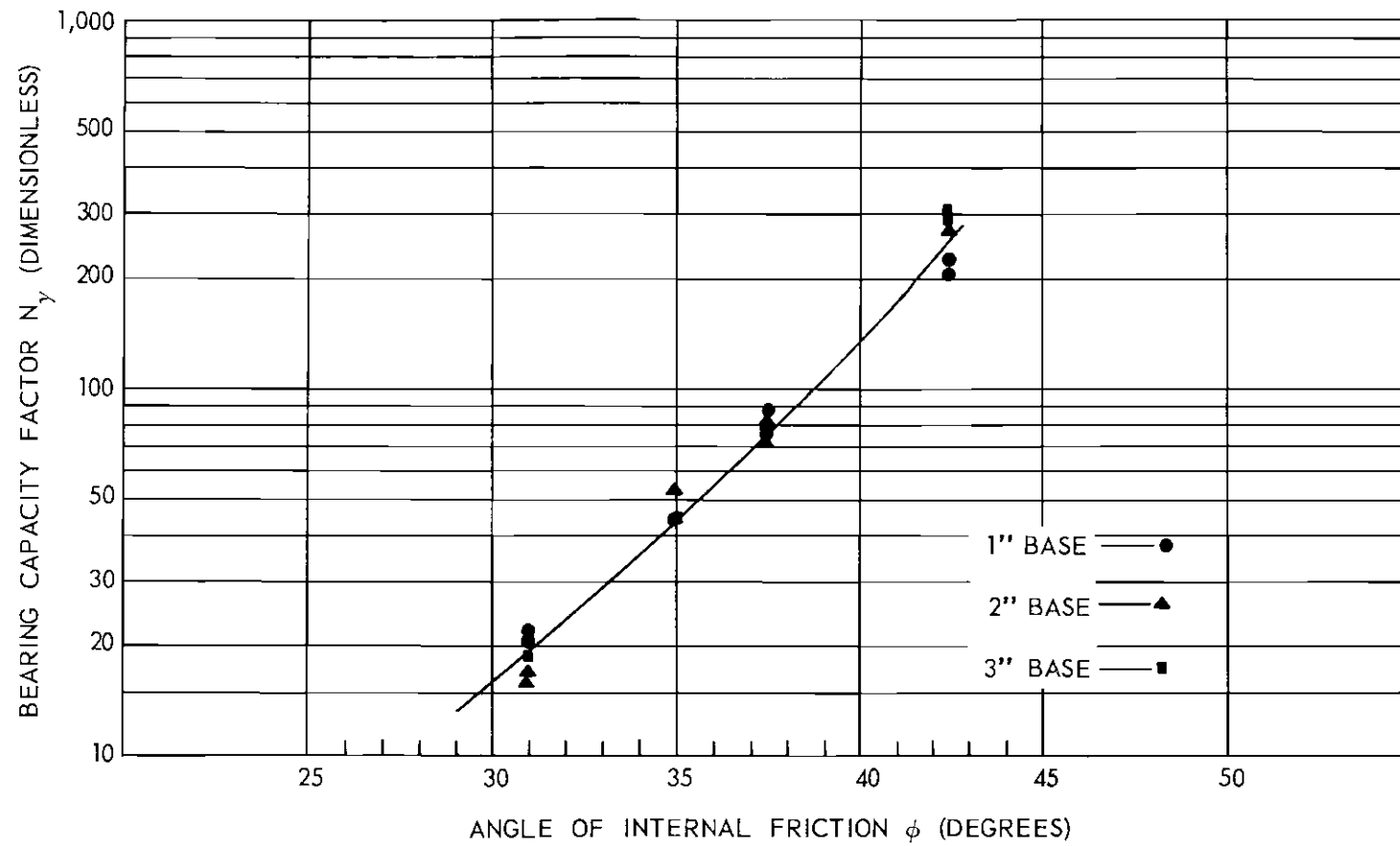


Figure 12. Results of Surface Plate Load Test Giving the Bearing Capacity Factor ( $N_\gamma$ ) as a Function of the Angle of Internal Friction ( $\phi$ ).

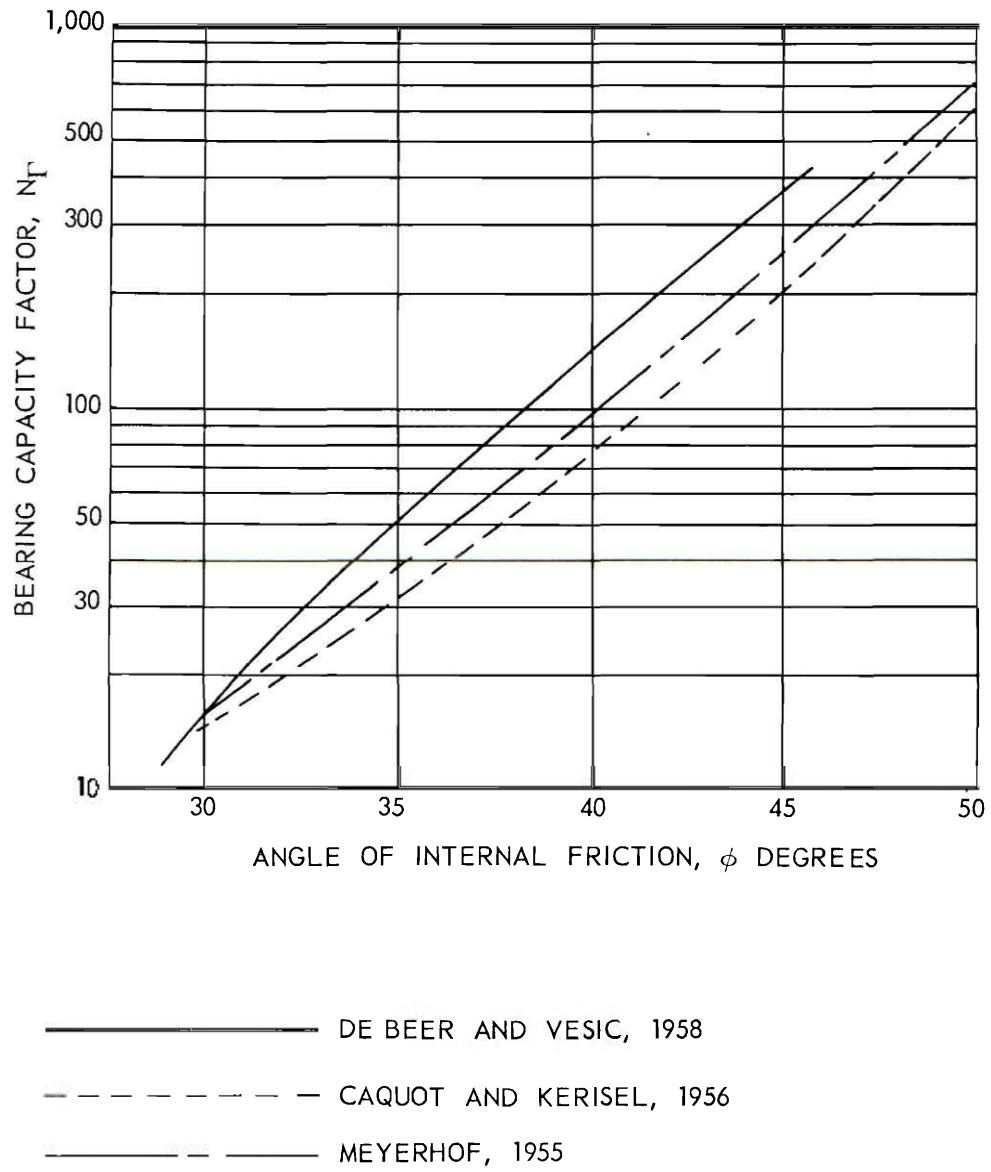


Figure 13. Comparison of  $N_\gamma$  Values for Surface Foundations.

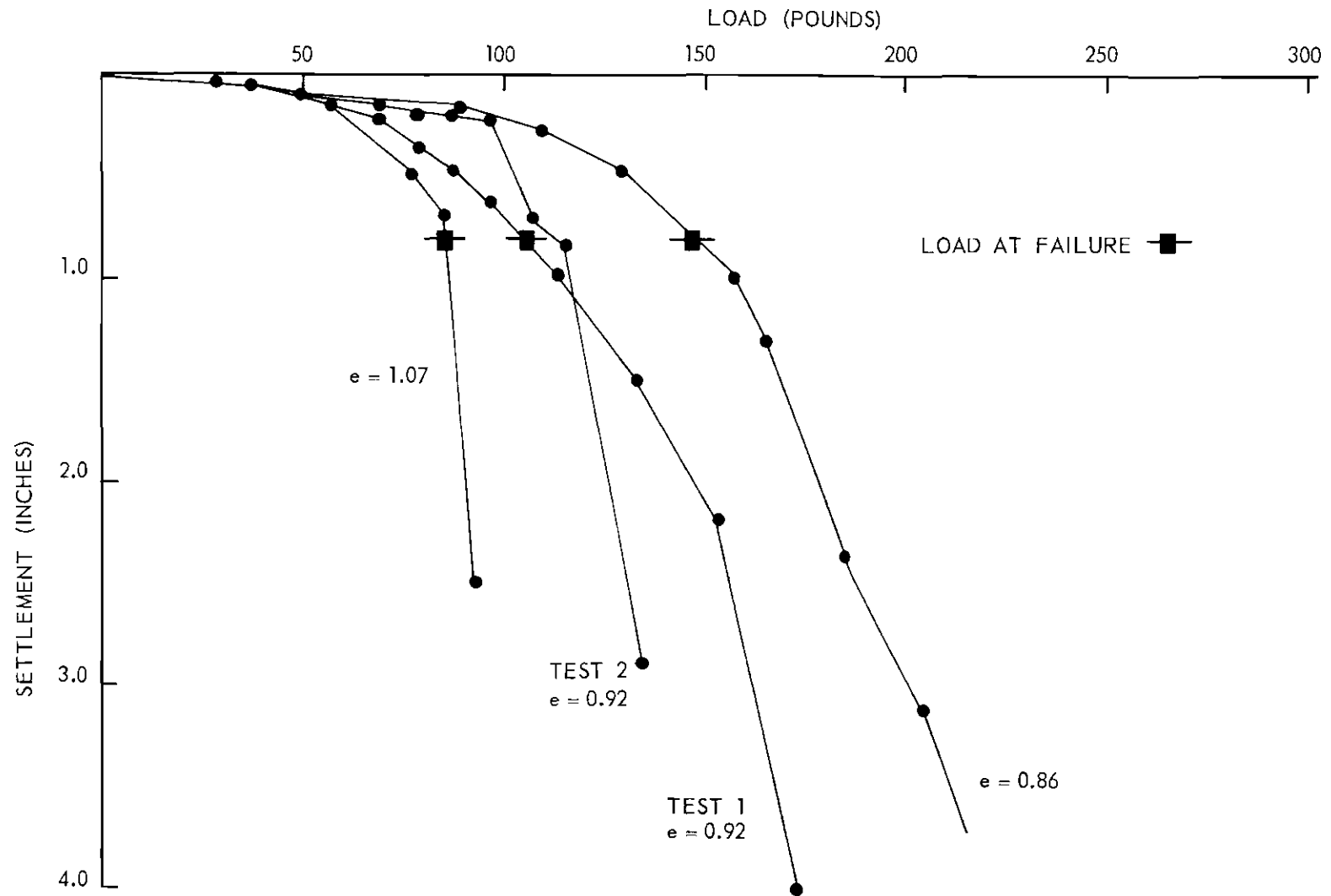


Figure 14. Load Settlement Curves (2" Footings Series II).



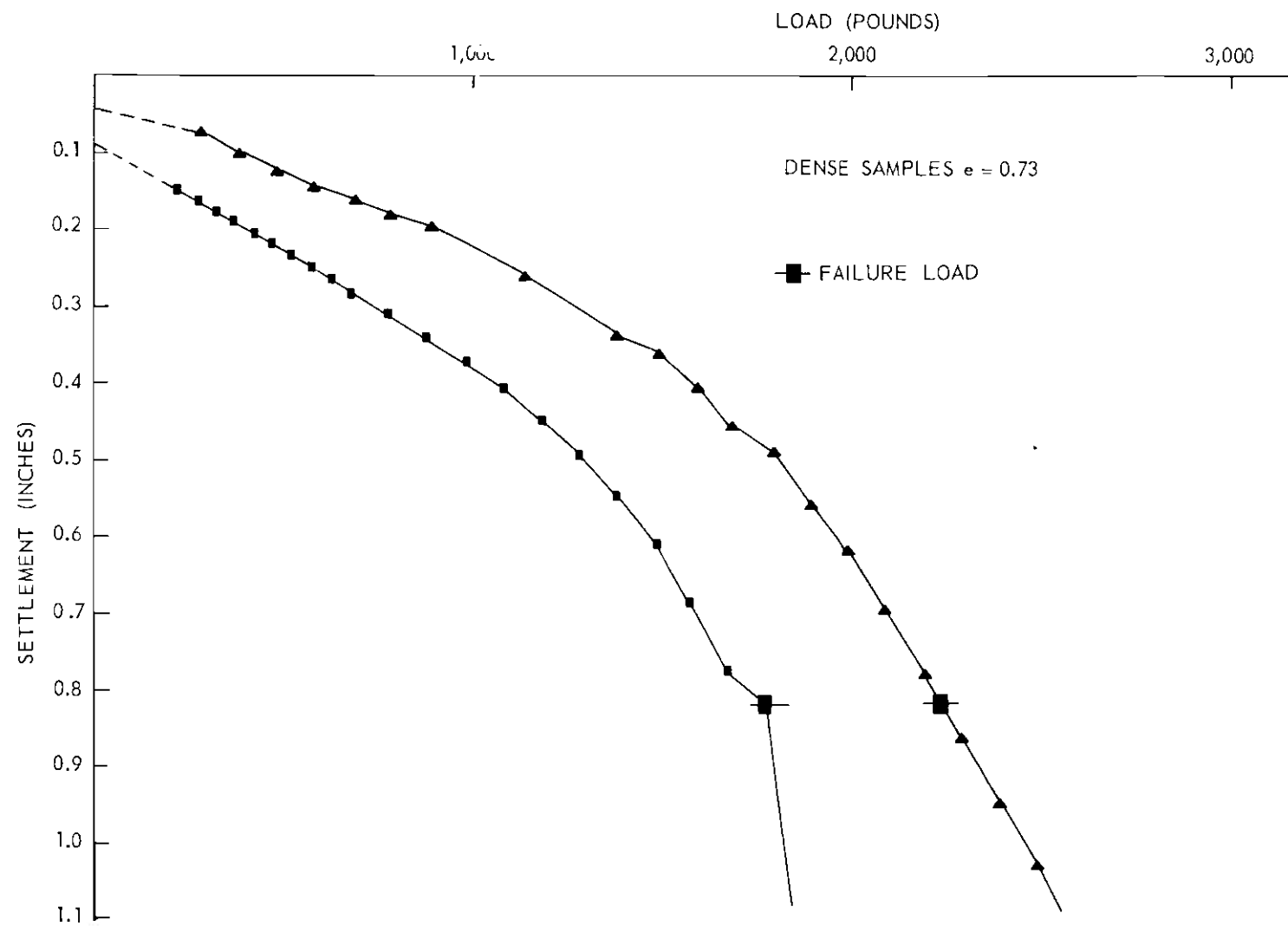


Figure 15. Load Settlement Curves (2" Footings Series II).

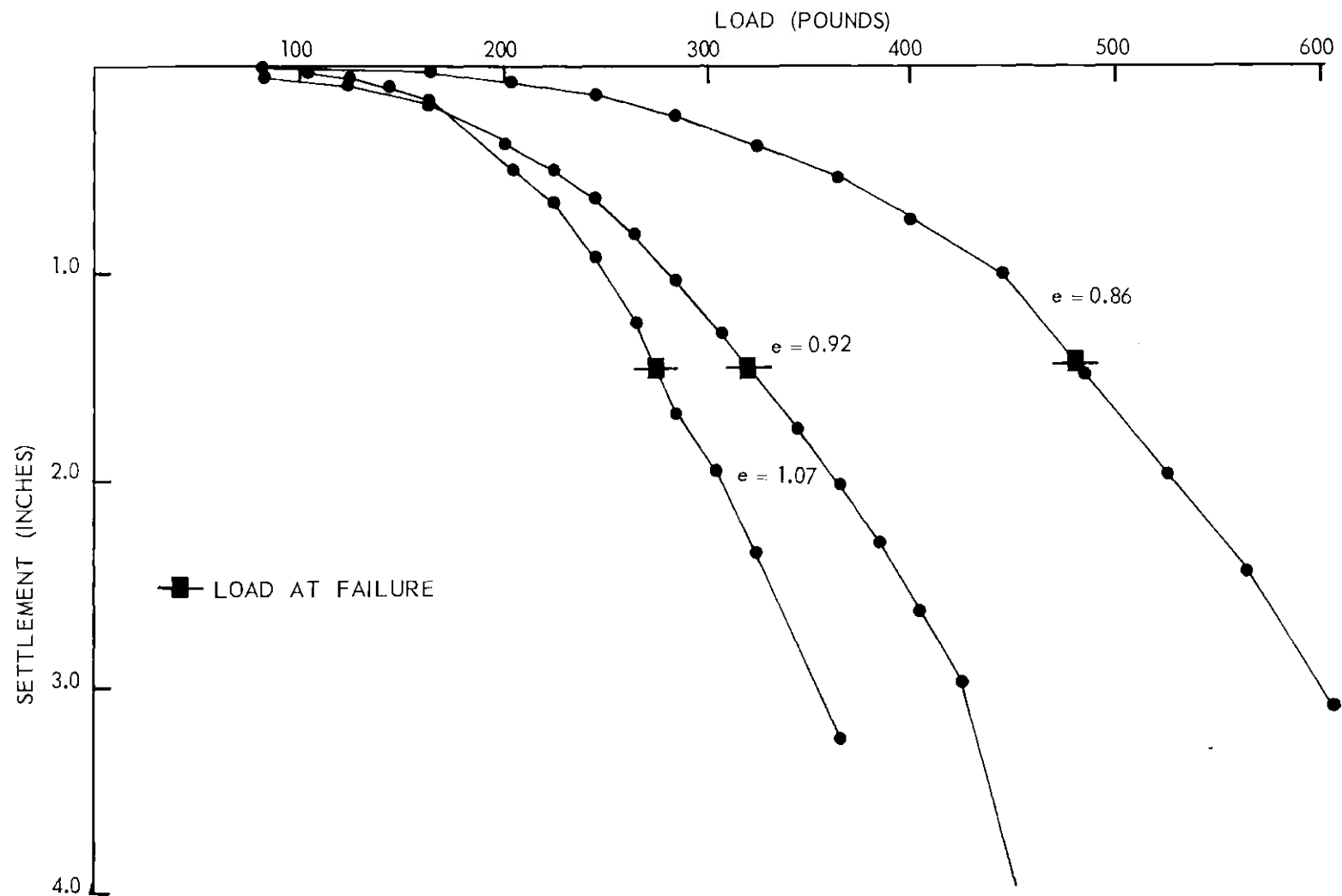


Figure 16. Load Settlement Curves (3" Footings Series II).

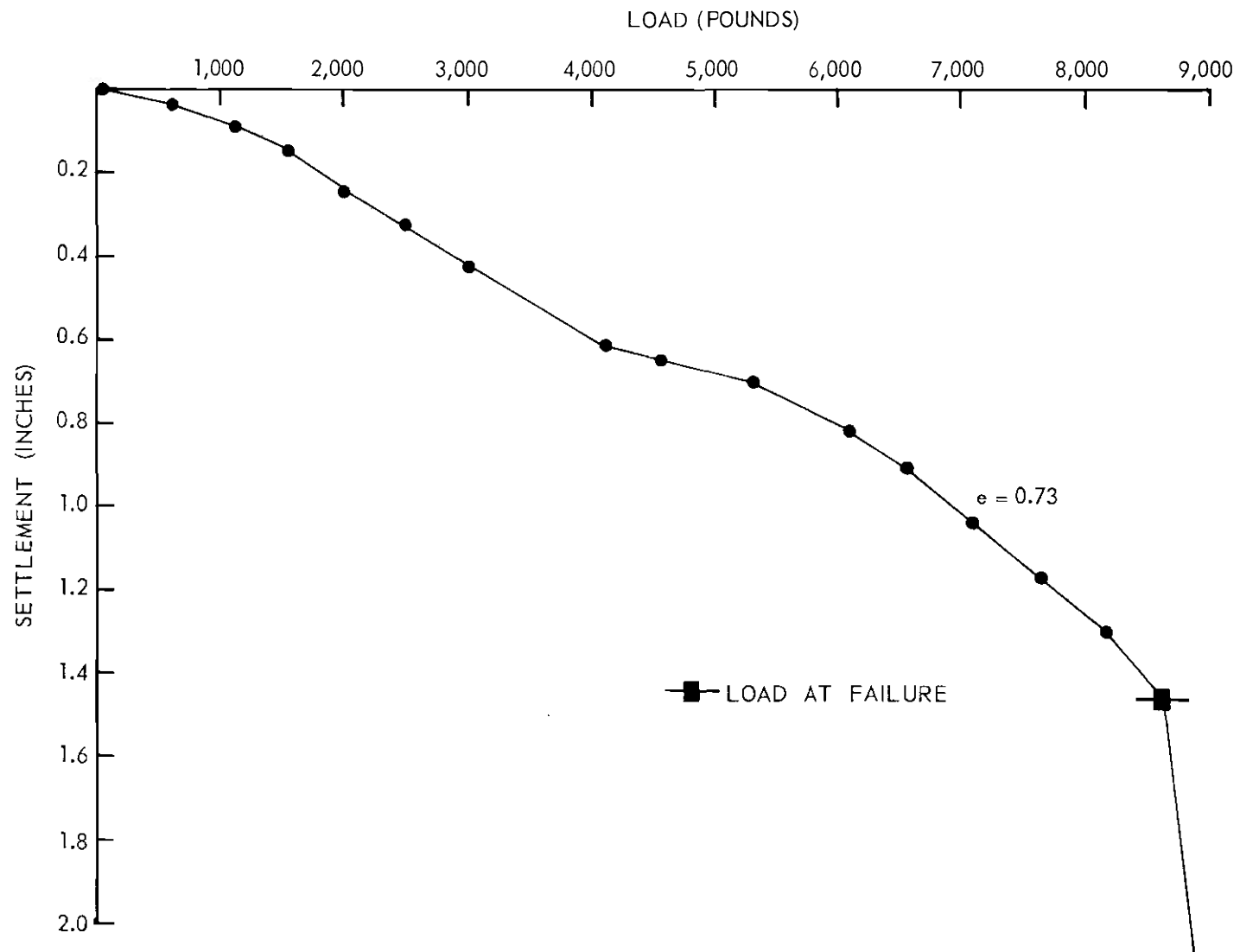


Figure 17. Load Settlement Curve (3" Footing Series II).

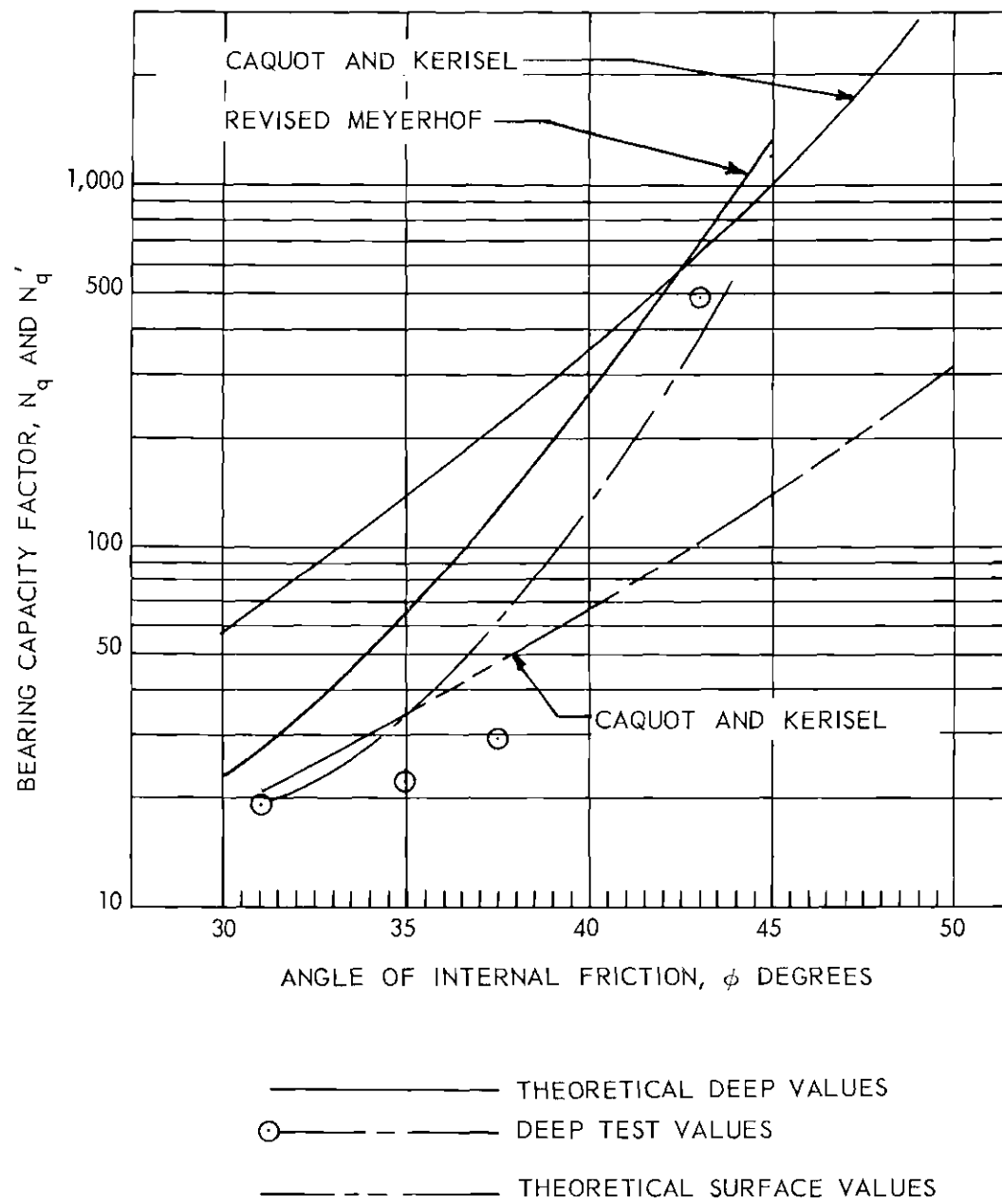


Figure 18. Theoretical and Test Values of  $N_q$  and  $N'_q$ .

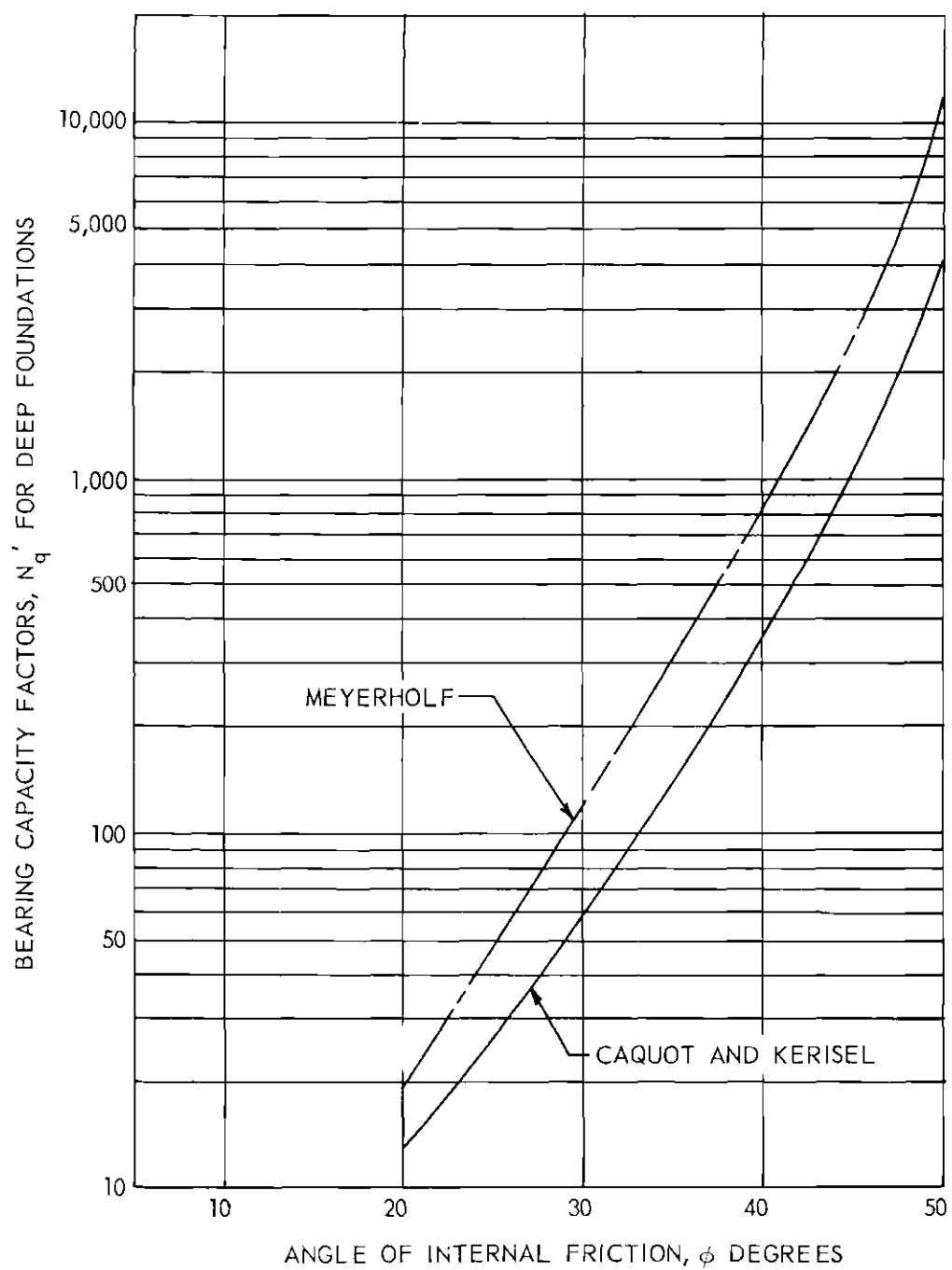


Figure 19. Comparison of Theoretical  $N'_q$  Values.

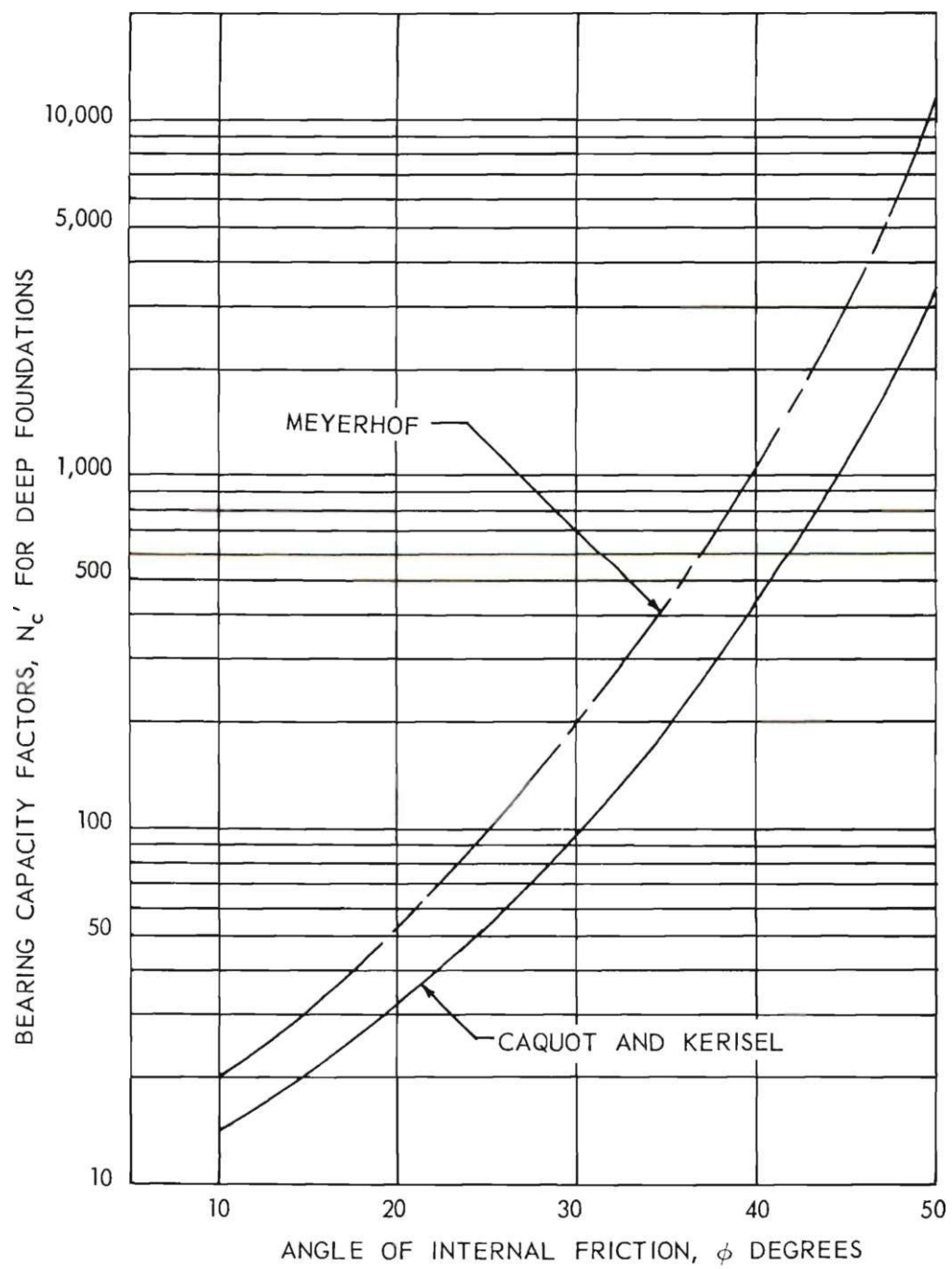


Figure 20. Comparison of Theoretical  $N'_c$  Values.

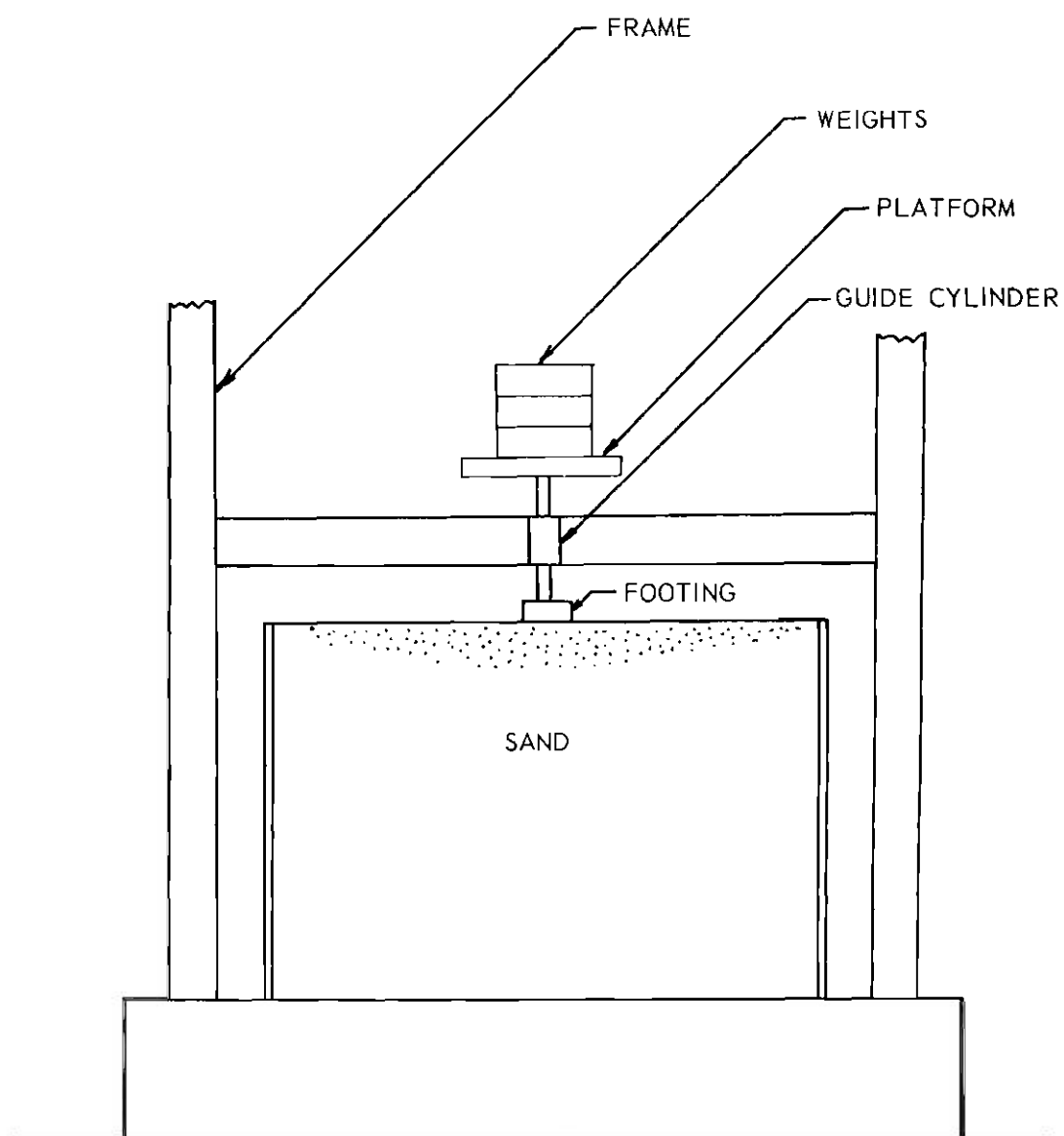


Figure 21. Large Surface Loading Apparatus.

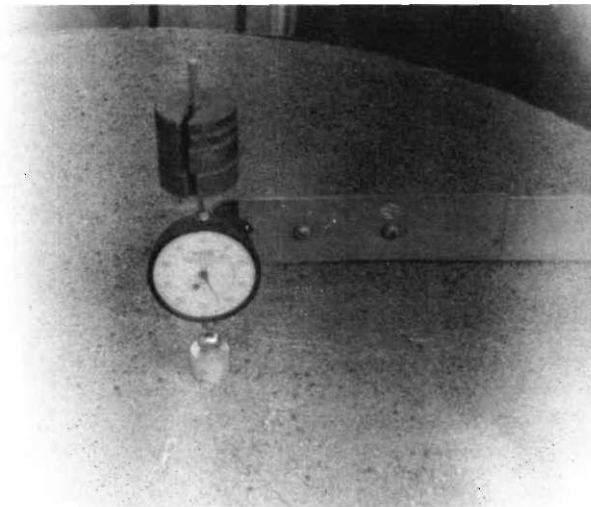


Figure 22. Small Surface Loading Apparatus.

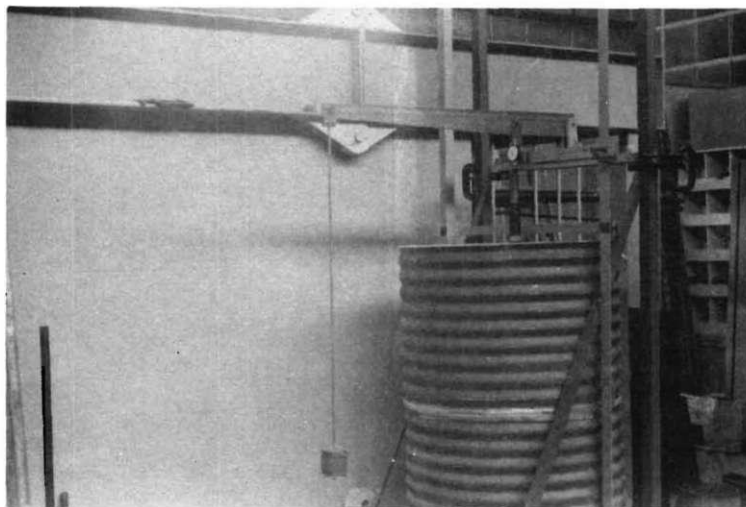


Figure 23. Small Lever Apparatus for Deep Load Testing.



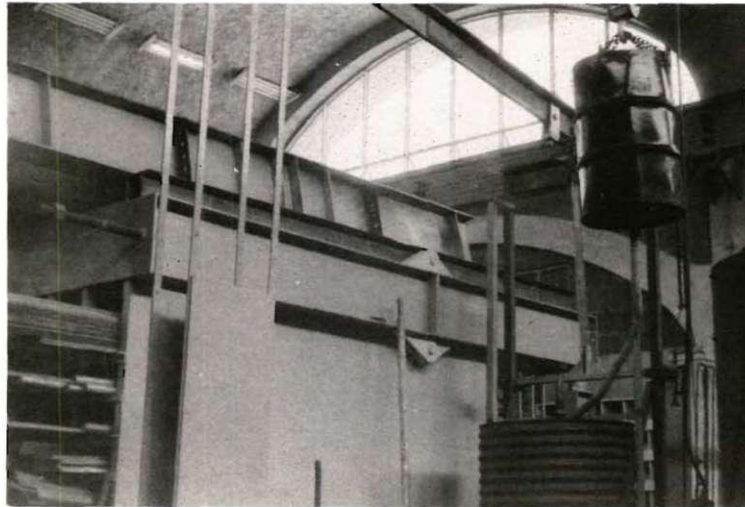


Figure 24. Apparatus for Conducting Deep Loading Tests.



Figure 25. Charging the Bin for a Deep Load Test.

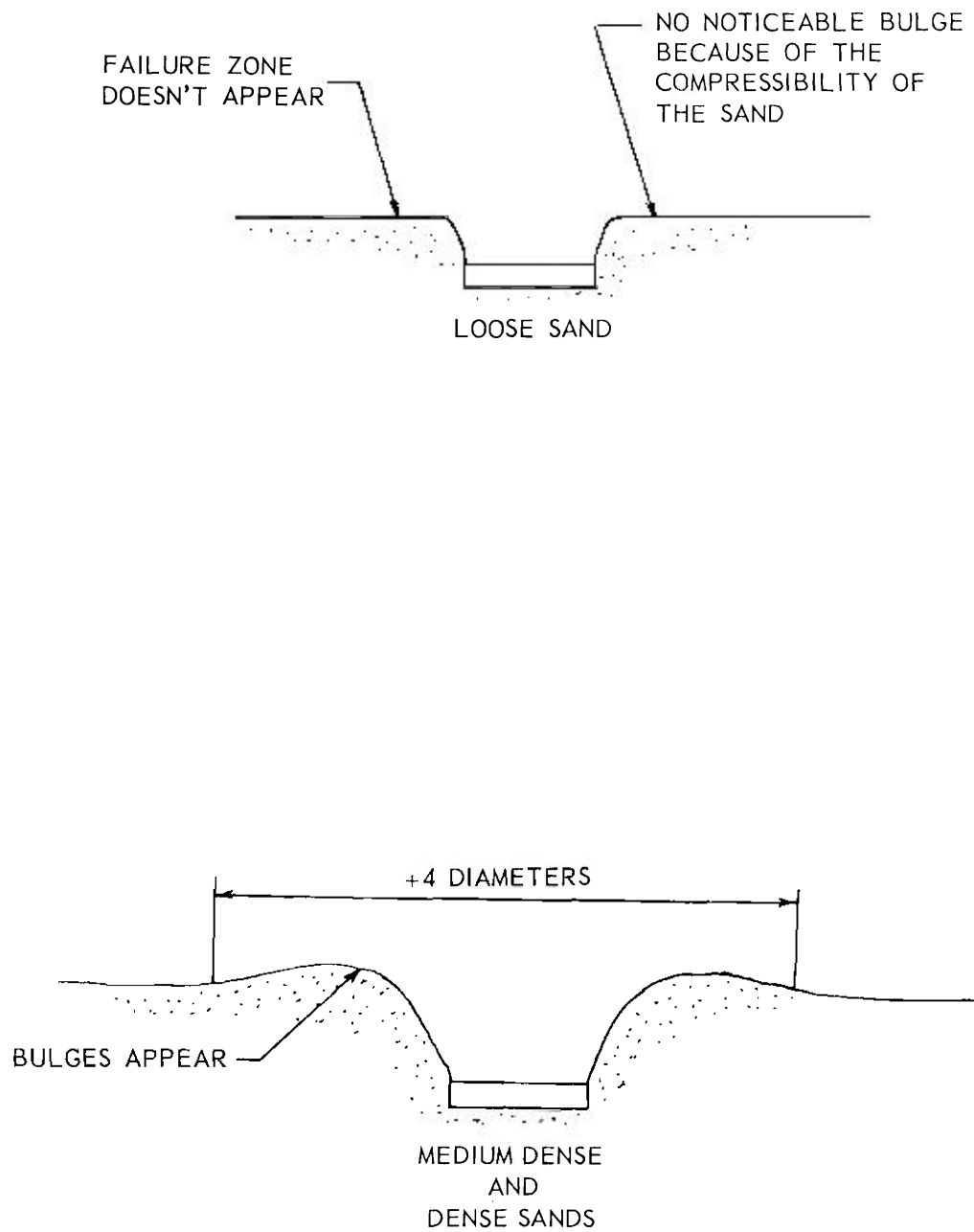


Figure 26. Cross Sections Across the Center of the Footing After Failure has Occurred.

## REFERENCES CITED

1. Terzaghi, K., Theoretical Soil Mechanics, 8th ed. New York: John Wiley and Sons, Inc., 1943, pp. 118-129.
2. Meyerhof, G. G., "An Investigation of the Bearing Capacity of Shallow Footings on Dry Sand," Proceedings of the Second International Conference on Soil Mechanics, 1, (1948), 237-243.
3. Meyerhof, G. G., "Influence of Roughness of Base and Ground Water Conditions on the Ultimate Bearing Capacity of Foundations," Geotechnique, 3, (1955), 227-242.
4. DeBeer, E. E. and A. B. Vesic, "Etude experimentale de la capacite portante du sable sous des fondations directes etablies en surface," Annales des Travaux Publics de Belgique, 3, (1958), 1-47.
5. Terzaghi, op. cit., pp. 118-134.
6. Meyerhof, G. G., "The Ultimate Bearing Capacity of Foundations," Geotechnique, 2, (1951), no. 4, 301-332.
7. Jaky, J., "On the Bearing Capacity of Piles," Proceedings of the Second International Conference on Soil Mechanics, 1, (1948), 100-103.
8. Ibid., pp. 301-332.
9. Caquot, A. and J. Kerisel, Traite de Mecanique des sols, 3rd ed. Paris: Gauthier-Villars, 1949, p. 434.
10. DeBeer, op. cit., p. 1.
11. Meyerhof, G. G., "The Ultimate Bearing Capacity," 301-332.
12. Terzaghi, op. cit., pp. 118-134.
13. Meyerhof, G. G., "The Ultimate Bearing Capacity," 301-332.
14. Terzaghi, op. cit., pp. 118-134.
15. DeBeer, op. cit., p. 1.

## OTHER REFERENCES

1. Mizuno, T., "On the Bearing Power of Soil in a Two Dimensional Problem," Proceedings of the Second International Conference on Soil Mechanics, 3, (1948), 44-48.
2. Mizuno, T., "On the Bearing Power of Soil Under a Uniformly Distributed Circular Load," Proceedings of the Third International Conference on Soil Mechanics, 1, (1953), 446-449.
3. Brinch Hansen, J., "General Report," Proceedings of the Fourth International Conference on Soil Mechanics, 2, (1957), 441-447.